2000

Kinetics and mechanisms of the oxidation of rhenium(V) oxo and thiolato complexes by alkyl hydroperoxides and orthoquinones

Kimberly Ann Brittingham
Iowa State University

INFORMATION TO USERS

This manuscript has been reproduced from the microfilm master. UMI films the text directly from the original or copy submitted. Thus, some thesis and dissertation copies are in typewriter face, while others may be from any type of computer printer.

The quality of this reproduction is dependent upon the quality of the copy submitted. Broken or indistinct print, colored or poor quality illustrations and photographs, print bleedthrough, substandard margins, and improper alignment can adversely affect reproduction.

In the unlikely event that the author did not send UMI a complete manuscript and there are missing pages, these will be noted. Also, if unauthorized copyright material had to be removed, a note will indicate the deletion.

Oversize materials (e.g., maps, drawings, charts) are reproduced by sectioning the original, beginning at the upper left-hand corner and continuing from left to right in equal sections with small overlaps.

Photographs included in the original manuscript have been reproduced xerographically in this copy. Higher quality 6" x 9" black and white photographic prints are available for any photographs or illustrations appearing in this copy for an additional charge. Contact UMI directly to order.

Kinetics and mechanisms of the oxidation of rhenium(V) oxo and thiolato complexes

by alkyl hydroperoxides and orthoquinones

by

Kimberly Ann Brittingham

A dissertation submitted to the graduate faculty

in partial fulfillment of the requirements for the degree of

DOCTOR OF PHILOSOPHY

Major: Inorganic Chemistry

Major Professor: James H. Espenson

Iowa State University

Ames, Iowa

2000

ii

Graduate College

Iowa State University

This is to certify that the Doctoral dissertation of

Kimberly Ann Brittingham

has met the dissertation requirements of Iowa State University

Signature was redacted for privacy.

Major Professor

Signature was redacted for privacy.

For the Major Program

Signature was redacted for privacy.

For the Graduate College

To

Joseph C. Welteroth

Clifton W. Pusey

Eva B. Pusey

Kathryn G. Bunting

William W. Brimer

Thank you for so many wonderful memories.

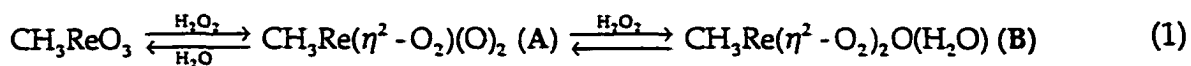I'll never forget you.

TABLE OF CONTENTS

GENERAL INTRODUCTION

Methyltrioxorhenium(VII) and Methyldioxorhenium(V)

The area of research concerning high valent rhenium complexes with strongly π-donating ligands such as oxygen or nitrogen atoms has been explored in depth over the past few decades. One particular complex that has received much attention is a rhenium(VII) complex, methyltrioxorhenium (CH_3ReO_3 or MTO), because it can be used as a catalyst with hydrogen peroxide to carry out a multitude of oxidation reactions.[1] The active species in these oxidations are η^2-peroxo rhenium(VII) complexes (eq 1) which are formed by condensation reactions.[2-5] The equilibrium reactions of MTO and hydrogen peroxide have been studied in depth.[3,4,6,7]

$$CH_3ReO_3 \xrightleftharpoons[H_2O]{H_2O_2} CH_3Re(\eta^2 - O_2)(O)_2 \text{ (A)} \xrightleftharpoons{H_2O_2} CH_3Re(\eta^2 - O_2)_2O(H_2O) \text{ (B)} \qquad (1)$$

One of the concerns in the area of catalysis is the integrity of the catalyst. CH_3ReO_3 undergoes irreversible decomposition in the presence of H_2O_2. The decomposition has been studied and the two pathways involve nucleophilic attack on the rhenium by either hydroperoxide anion, HO_2^-, (eq 2)[2] or hydroxide, HO^- (eq 3)[2,8].

$$HO_2^- + CH_3ReO_3 \rightarrow CH_3OH + ReO_4^- \qquad (2)$$

$$OH^- + CH_3ReO_3 \rightarrow CH_4 + ReO_4^- \qquad (3)$$
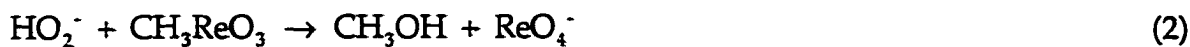
The rhenium-oxygen bonds of MTO are strong (464 kJ mol^{-1}).[9] Consequently, its reduction requires an oxygen atom acceptor that has a strong element-oxygen bond.[9] Either phosphines (free or polymer supported) or hypophosphorous acid

(eq 4) will serve as this oxygen acceptor.[8-10] The metastable, reduced form of MTO is called methyldioxorhenium (CH_3ReO_2 or MDO).

$$CH_3ReO_3 + H_3PO_2 \rightarrow CH_3ReO_2 + H_3PO_3 \tag{4}$$

The reaction of MTO with H_3PO_2 has been studied in acidic aqueous solution. The rate constant for the formation of MDO is 2.8×10^{-2} L mol^{-1} s^{-1} at 25°C.[9] Since MDO is a strong reducing agent, it has the ability to abstract an oxygen atom from substrates such as organic oxides, oxoanions and oxo-metal species.[9]

Alkyl Hydroperoxides

Olefin epoxidation catalysis has not been observed in solutions of alkyl hydroperoxides and methyltrioxorhenium.[11] These peroxides obviously do not activate MTO in the same manner as hydrogen peroxide. This is surprising because in most studies involving catalytic epoxidations carried out by d^0 metals, the mechanism is the same whether the oxidant is H_2O_2 or ROOH.[12]

There have been many studies of the reactions of alkyl hydroperoxides with metal complexes. Alkyl hydroperoxides undergo either homolytic or heterolytic cleavage when they react with metal centers. In the homolytic case, the O-O bond is split and radicals are generated as reactive intermediates. In the heterolytic case either the R-O or H-O bond is broken.[13]

Smurova et al. reported that MTO decomposes cumyl hydroperoxide, $C_6H_5(CH_3)_2COOH$, by heterolytic autocatalysis in chlorobenzene, stating that if radicals are involved, they take part in less than 1% of the process.[14] Conversely, in aqueous solution, alkyl hydroperoxides are cleaved homolytically after binding to

MTO and concurrent decomposition occurs.[15] This study assisted in the evaluation of the decomposition of MTO in solutions of H_2O_2, as mentioned earlier.

Also, alkyl hydroperoxides have the capacity to heterolytically oxidize MDO (eq 5).

$$ROOH + CH_3ReO_2 \rightarrow ROH + CH_3ReO_3 \tag{5}$$
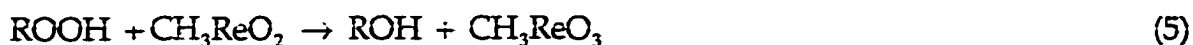
When hydrogen peroxide (R = H) is used as the oxidizing agent in the above reaction, it proceeds all the way to the η^2-peroxo complexes **A** and **B** (eq 1). The triangular peroxidic moiety is not formed upon activation of alkyl hydroperoxides with the rhenium in MDO, and thus their use has allowed an investigation into the kinetics of eq 5.[15]

Oxidation of Rhenium(V) by Molecular Oxygen

There is evidence that MDO can activate oxygen to form an η^2-peroxo complex, which can subsequently oxidize tri(p-tolyl)phosphine.[16] In effect, MTO and MDO complexes have been transformed into the same η^2-peroxo species, **A**, via two different methods: the condensation reaction of MTO with H_2O_2 (eq 1) and the oxidation of MDO by O_2 (eq 6)

$$CH_3ReO_2 + O_2 \rightarrow CH_3ReO_2(\eta^2 - O_2) \tag{6}$$
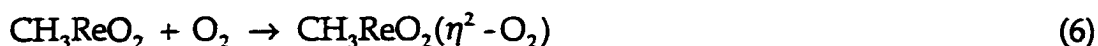
The proposed mechanism for oxygen activation by MDO is complicated by phosphine-MDO binding equilibria.[16]

Quinones and their Derivatives as Ligands for Rhenium

In an effort to learn more about the oxidation of Re(V) without the complication of net O-atom transfer, a different set of ligands was explored. The general term used for these ligands is quinones. In coordination compounds they

are usually bound as either semiquinones or catecholates, which are the one- and two-electron reduced forms.
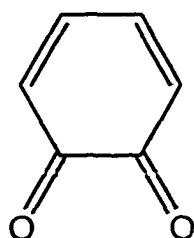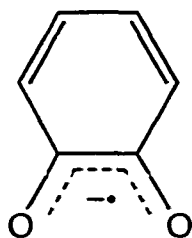
Quinone   Semiquinone   Catecholate
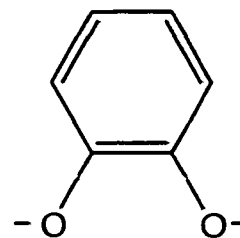
One reason that inorganic chemists have been interested in catecholates is their biological significance. An iron siderophore, enterobactin, consists of three ortho-catecholate groups.[17] Catecholamines such as epinephrine, norepinephrine and dopamine are ortho-catechols that are used as neurotransmitters in the body.[18] Catecholate complexes of ^{186}Re and ^{99m}Tc also have potential uses in the area of radiopharmaceuticals.[19-25]

There are examples of quinone complexes for almost every metal. Two comprehensive reviews about the structure and reactivity of these transition metal complexes have been published.[26,27] Evidence suggests that whichever form they adopt as ligands, it is appropriate to view their electronic structures as localized even though the levels of the metal d orbitals and the quinone π^* electronic levels are close in energy. Pierpont has suggested the following diagram to explain the charge distribution in metal-quinone complexes based on the energy of their respective frontier orbitals.[26]
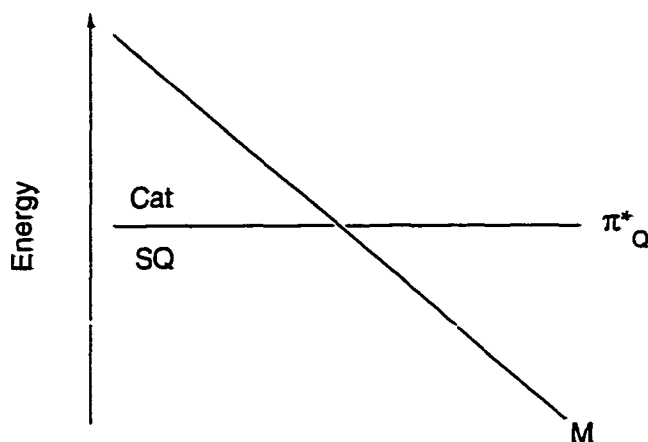
If the metal d orbitals are higher in energy than the quinone π^* orbitals, the charge will reside on the ligand and they will bind as catecholates. If, on the other hand, the metal orbitals are at a lower energy than the ligand frontier orbitals, the ligands will coordinate as semiquinones so that more electron density will remain on the metal. When the energies of the orbitals lie in the region close to where the lines intersect, valence tautomerism has been observed. For example, when purple crystals of $Mn^{IV}(3,5\text{-}DBCat)_2(Py)_2$ were dissolved in toluene at room temperature, the solution turned green due to the presence of $Mn^{II}(3,5\text{-}DBSQ)_2(Py)_2$.[28] These two species are in a tautomeric equilibrium between 230 and 300 K in toluene.

The characterization of quinone complexes has relied largely on structural investigations. Quinone C-O and C-C (the bond between the carbons attached to the oxygens) bond lengths are sensitive to the charge on the ligand. For example the typical C-O lengths are 1.337-1.387 Å for catecholates and 1.272-1.312 Å for semiquinones. The trend in C-C bonds is the opposite; 1.348-1.415 Å for catecholates and 1.42-1.453 Å for semiquinones. EPR has also been an essential tool in identifying the semiquinone radical species.

Several high valent rhenium-catecholato complexes have been reported in the literature. Some examples of Re(V) complexes with a chelating catecholate ligand are [ReO(L)(PPh$_3$)$_2$X] (X = Cl, I, H$_2$L = catechol or substituted catechol),[29] [NBu$^n_4$][ReO(OPPh$_3$)(L)$_2$](L = Cl$_4$Cat, Br$_4$Cat),[29] [Me$_4$N][ReO(Cat)$_2$(PPh$_3$)], [Me$_4$N][ReO(cat)$_2$(PPh$_3$)],[25] and [Re(η^5-C$_5$Me$_5$)(L)$_2$] (L = Cl$_4$Cat, PCat).[30] The dark purple Re(DBCat)$_3$ is a rare example of an air and water stable Re(VI) complex.[31] EPR studies have proved that the unpaired electron on Re(DBCat)$_3$ resides on the d^1 metal as opposed to a semiquinone ligand. The crystal structure of an oxo-catecholato Re(VII) complex, [Me$_4$N][ReO$_2$(cat)$_2$], was determined by Dilworth and coworkers.[32] The geometry about the Re in this complex is distorted octahedral with the two terminal oxygens occupying positions *cis* to each other. These oxo groups create strong *trans*-influence on the catecholate ligands causing them to be asymetrically coordinated. Chelated rhenium-semiquinone complexes do exist, but only when rhenium is in a low oxidation state such as Re(CO)$_4$(DBSQ) [33] and Re(CO)$_3$PPh$_3$(DTBQ).[34]

Two similar Re(VII) catecholate complexes have been synthesized using methods analogous to the reactions of MTO and MDO with H$_2$O$_2$ (eq 1) and O$_2$ (eq 6) respectively. The first method consisted of a condensation reaction of MTO with catechol to form CH$_3$Re(O)$_2$(1,2-O$_2$C$_6$R$_4$)(NC$_5$H$_5$).[35] The second complex, CH$_3$Re(O)$_2$(9,10-O$_2$C$_{14}$H$_8$)(NC$_5$H$_5$), was prepared by the oxidation of MDO (prepared in situ from MTO and polymer supported triphenylphosphine) by phenanthrenequinone.[35] Pyridine was necessary for the precipitation of both purple solids.

Dithiolato Complexes of Rhenium(V)

A different set of stable and isolable Re(V) complexes has been employed in the analysis of quinone binding equilibria. A novel dithiolato rhenium(V) dimer has been previously prepared according to eq 7.[36]

$$\tag{7}$$
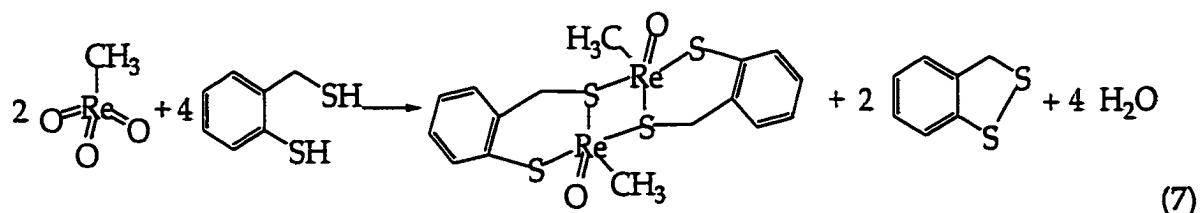
Many different monodentate ligands, such as pyridines, phosphines and simple anions, are capable of monomerizing this dimer (eq 8).[36-38]

$$\{MeORe(dithiolato)\}_2 + 2 L \rightleftarrows 2 MeORe(dithiolato)Py \tag{8}$$

The ligand substitution of these monomer ligand complexes has also been studied in depth.[38,39] A second monomer-ligand complex MeORe(edt)PPh$_3$ has since been synthesized by an alternate route.[40] The ethanedithiol dimer, $\{MeORe(edt)\}_2$, has been prepared from Re$_2$(CH$_3$)$_2$(O)$_2$(SPh)$_4$,[35] ethanedithiol and methyl sulfide.[41] The equilibrium data of the monomerization of this dimer by electron donating pyridine ligands (eq 8) will be presented.

When phenanthrenequinone reacts with either of the monomer-pyridine complexes, a ligand substitution reaction occurs. In fact, the system reaches equilibrium where the quinone and the pyridine ligand are interchanging (eq 9).

$$M-Py + PQ \rightleftarrows M-PCat + Py \tag{9}$$

PCat is phenanthrenecatechol. When DBQ is used instead of PQ, the reaction is faster and goes to completion. These systems have been studied in depth and a mechanism has been proposed based on the experimental data. Although substitution reactions are widely used in the synthesis of metal-catecholate and metal-semiquinone complexes, no kinetic or thermodynamic study has previously been carried out.

Dissertation Organization

This dissertation consists of two chapters. Chapter 1 corresponds to a manuscript to be submitted to *Inorganic Chemistry*. Chapter 2 has been published in *Inorganic Chemistry*. Each chapter is self-contained with its own equations, figures, tables, schemes, charts, and references. The General Conclusions section follows the last chapter. With the exception of the GC-MS experiment (performed with Dr. Kamel Harrata) and the electrospray mass spectrometry experiment (performed with Sahana Mollah) from Chapter 2, all the work in this dissertation was performed by the author, Kimberly A. Brittingham.

References

1)Espenson, J. H.; Abu-Omar, M. M. *Adv. Chem. Ser.* **1997**, *253*, 99.

2)Abu-Omar, M. M.; Hansen, P. J.; Espenson, J. H. *J. Am. Chem. Soc.* **1996**, *118*, 4966.

3)Espenson, J. H.; Pestovsky, O.; Houston, P.; Staudt, S. *J. Am. Chem. Soc.* **1994**, *116*, 2869.

4)Yamazaki, S.; Espenson, J. H.; Huston, P. *Inorg. Chem.* **1993**, *32*, 4683.

5)Herrmann, W. A.; Fischer, R. W.; Scherer, W.; Rauch, M. U. *Angew. Che., Int. Ed. Engl.* **1993**, *32*, 1157.

6)Zhu, Z.; Espenson, J. H. *J. Org. Chem.* **1995**, *60*, 1326.

7)Pestovsky, O.; van Eldik, R.; Huston, P.; Espenson, J. H. *J. Chem. Soc. Dalton Trans.* **1995**, 133.

8)Zhu, Z.; Espenson, J. H. *J. Mol. Catal.* **1995**, *103*, 87.

9)Abu-Omar, M. M.; Appelman, E. H.; Espenson, J. H. *Inorg. Chem.* **1996**, *35*, 7751.

10)Herrmann, W. A.; Roesky, P. W.; Wang, M.; Scherer, W. *Organometallics* **1994**, *13*, 4531.

11)Herrmann, W. A.; Fischer, R. W.; Marz, D. W. *Angew. Chem. Int. Ed. Engl.* **1991**, *30*, 1638.

12)Mimoun, H. *Israel J. Chem.* **1983**, *23*, 451.

13)Sheldon, R. A.; Kochi, J. K. *Metal-Catalyzed Oxidations of Organic Compounds*; Academic: New York, 1981.

14)Smurova, L. A.; Kholopov, A. B.; Nikitin, A. V.; Brin, E. F.; Rubailo, V. L. *Kinet. and Catal.* **1996**, *37*, 361.

15)Brittingham, K. A.; Espenson, J. H. *Inorg. Chem.* **1999**, *38*, 744-750.

16)Eager, M. D.; Espenson, J. H. *Inorg. Chem.* **1999**, *38*, 2533.

17)Lippard, S. J.; Berg, J. M. *Principles of Bioinorganic Chemistry*; University Science Books: Mill Valley, CA, 1994, pp 71-72.

18)Campbell, N. A. *Biology*; 2nd ed.; The Benjamin/Cummings Publishing Company, Inc.: Redwood City, CA, 1990, pp 925, 993.

19)Abrams, M. J.; Juweid, M.; ten Kate, C. I.; Schwartz, D. A.; Hauser, M. M.; Gaul, F. E.; Fuccello, A. J.; Rubin, R. H.; Strauss, H. W.; Fischman, A. J. *J. Nucl. Med.* **1990**, *31*, 2022.

20)Abrams, M. J.; Shaikh, S. N.; Zubeita, J. *Inorg. Chim. Acta* **1990**, *173*, 133.

21)Abrams, M. J.; Larsen, S. K.; Zubieta, J. *Inorg. Chim. Acta* **1990**, *171*, 133.

22)Abrams, M. J.; Chen, Q.; Shaikh, S. N.; Zubieta, J. *Inorg. Chim. Acta* **1990**, *176*, 11.

23)Abrams, M. J.; Larsen, S. K.; Shaikh, S. N.; Zubieta, J. *Inorg. Chim. Acta* **1991**, *185*, 7.

24)Davison, A.; DePamphilis, B. V.; Jones, A. G.; Franklin, K. J.; Lock, C. J. L. *Inorg. Chim. Acta* **1987**, *128*, 161.

25)Kettler, P. B.; Chang, Y.-D.; Zubieta, J.; Abrams, M. J. *Inorganica Chimica Acta* **1994**, *218*, 157.

26)Pierpont, C. G.; Lange, C. W. *Progress in Inorganic Chemistry* **1994**, *41*, 331.

27)Pierpont, C. G.; Buchanan, R. M. *Coordination Chemistry Reviews* **1981**, *38*, 45.

28)Lynch, M. W.; Hendrickson, D. N.; Fitzgerald, B. J.; Pierpont, C. G. *J. Am. Chem. Soc.* **1984**, *106*, 2041.

29)Edwards, C. F.; Griffith, W. P.; White, A. J. P.; Williams, D. J. *J. Chem. Soc., Dalton Trans.* **1992**, 957.

30)Herrmann, W. A.; Kusthardt, U.; Herdtweck, E. *J. Organomet. Chem.* **1985**, *294*, C33.

31)deLearie, L. A.; Pierpont, C. G. *J. Am. Chem. Soc.* **1986**, *108*, 6393.

32)Dilworth, J. R.; Ibrahim, S. K.; Khan, S. R.; Hursthouse, M. B.; Karaulov, A. A. *Polyhedron* **1990**, *9*, 1323.

33)Creber, K. A. M.; Wan, J. K. S. *J. Am. Chem. Soc.* **1981**, *103*, 2101.

34)Cheng, C. P.; Wang, S. R.; Lin, J. C.; Wang, S.-L. *Journal of Organometallic Chemistry* **1988**, *349*, 375.

35)Takacs, J.; Cook, M. R.; Kiprof, P.; Kuchler, J. G.; Herrmann, W. A. *Organometallics* **1991**, *10*.

36)Jacob, J.; Guzei, I. A.; Espenson, J. H. *Inorg. Chem.* **1999**, *38*, 1040.

37)Lente, G.; Jacob, J.; Guzei, I. A.; Espenson, J. H. *Inorg. React. Mech.* , accepted.

38)Lente, G.; Espenson, J. H. *Inorg. Chem.* , submitted.

39)Lahti, D. W.; Espenson, J. H. *Submitted for publication* .

40)Lente, G.; Shan, X.; Guzei, I. A.; Espenson, J. H. *Inorg. Chem.* **2000**, *39*, 3572.

41)Shan, X.; Espenson, J. H. , unpublished information.

CHAPTER 1

THERMODYNAMICS, KINETICS AND MECHANISM OF THE REVERSIBLE

FORMATION OF OXORHENIUM(VII)-CATECHOLATE COMPLEXES

A paper submitted to Inorganic Chemistry[*]

Kimberly A. Brittingham and James H. Espenson

Abstract

Mononuclear Re(V) compounds, $MeReO(mtp)NC_5H_4X$, **3**, where $mtpH_2$ is 2-(mercaptomethyl)thiophenol, have been prepared from the monomerization of ${MeReO(mtp)}_2$ (**1**) by pyridines with electron-donating substituents in the para or meta position; X = 4-Me, 4-Bu^t, 3-Me, 4-Ph, and H. Analogous compounds, $MeReO(edt)N_5H_4X$, **4**, $edtH_2$ = 1,2-ethanedithiol, were prepared similarly. The equilibrium constants for the reaction, Dimer + 2 Py = 2 M–Py, are in the range $2.5–31.6 \times 10^2$. Both groups of monomeric compounds react with quinones (phenanthrenequinone, PQ, and 3,5-*tert*-butyl-1,2-benzoquinone, DBQ) displacing the pyridine ligand and forming Re(VII) catecholate complexes $MeReO(dithiolate)Pcat$ and $MeReO(dithiolate)DBCat$ (**5** & **6**). With PQ, the reaction M–Py + PQ = M–Pcat + Py is an equilibrium; values of K_Q for different Py ligands lie in the range 9.2–42.7 (mtp) and 3.2–11.2 (edt) at 298 K. These second-order rate constants (L mol^{-1} s^{-1}) at 25 °C in benzene were obtained for the

PQ reactions: k_f = (5.3-15.5) × 10^{-2} (mtp) and (6.6-16.4) × 10^{-2} (edt); k_r = (3.63-5.71) × 10^{-3} (mtp) and (14.7-22.0) × 10^{-3} (edt). The ranges in each case refer to the series of pyridine ligands, the forward rate constant being the largest for C_5H_5N, with the lowest Lewis basicity. The reactions of M–Py complexes with DBQ proceeded to completion. Values of k_f/L mol^{-1} s^{-1} fall in a narrow range, 4.02 (X = 4-Bu^t) - 8.4 (X = H) with the mtp dithiolate.

Introduction

The chemistry of Re(VII) complexes with strongly π-donating oxygen and nitrogen ligands has been of considerable recent interest. One particular compound that has been studied extensively is methyltrioxorhenium(VII) (MeReO$_3$ or MTO). Condensation reactions provide a means of derivatizing metal-oxo groups:

$$M=O + H_2Y \text{ (or 2 HZ)} \rightarrow H_2O + MY \text{ (or } MZ_2) \tag{1}$$

We have previously used this type of reaction to convert MTO into a dimeric dithiolato-Re(V) complex, 1, by reaction with dithiols.[1,2]

$$2\,MeReO_3 + 4\,mtpH_2 \rightarrow \{MeReO(mtp)\}_2 + 2\,RS\text{-}SR + 4\,H_2O \tag{2}$$
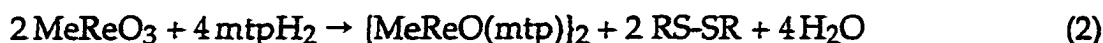
where mtpH$_2$ is 2-(mercaptomethyl)thiophenol and RS-SR its oxidation product, the cyclic disulfide. The dimer {MeReO(edt)}$_2$, 2 (edtH$_2$ = ethane-1,2-dithiol), is formed from Me$_2$Re$_2$O$_2$(SPh)$_4$, edtH$_2$ and methyl sulfide.[3] These compounds and their mononuclear counterparts formed by ligand (e.g., pyridine) addition to the dimers, MeReO(mtp)Py and MeReO(edt)Py, are proving to be effective catalysts

for oxygen transfer reactions.[3-5] Two factors are important. One is the Re(V)–Re(VII) transformation by O-atom uptake, and its reverse, these steps being the ones that accomplish oxygen-transfer. The second factor concerns the rates and mechanism of ligand substitution.[6,7] The reaction between oxorhenium(V) compounds and ortho-quinones addresses both of these issues while avoiding the complication of net oxygen-atom transfer.

Quinones and catechols are of considerable biological significance. Enterobactin, for example, is a siderophore consisting of three ortho-catecholate groups.[8] Catecholamines such as epinephrine, norepinephrine and dopamine are ortho-catechols that are used as neurotransmitters.[9] Catecholate complexes of oxotechnetium(V) have been studied as models for synthetic precursors to radiopharmaceutical proteins,[10-15] and thus ^{99m}Tc and ^{186}Re catecholates hold potential interest in nuclear medicine.[16]

Several high valent rhenium-catecholate complexes have been identified. Re(V) complexes include [ReO(Cat)(PPh$_3$)$_2$X] (X = Cl, I),[17] [ReO(Cat)$_2$(OPPh$_3$)]$^-$,[17] [ReO(Cat)$_2$(PPh$_3$)$_2$]$^-$,[16] and [Cp*Re(Cat)$_2$].[18] There is even one compound, [ReO{O(OH)C$_6$H$_4$}(S$_2$CNEt$_2$)$_2$], in which the catecholate binds in a monodentate fashion.[19] The dark purple compound, Re(DBCat)$_3$, is a rare example of a Re(VI) compound stable to air and water.[20,21] The crystal structure of [Me$_4$N] [ReO$_2$(Cat)$_2$] was determined.[22] Chelated rhenium-semiquinone complexes do

exist, but only when rhenium is in a low oxidation state such as $Re(CO)_4(DBSQ)$.[23]

The condensation reaction between MTO and catechol forms $CH_3Re(O)_2(1,2-O_2C_{14}H_8)(NC_5H_5)$.[24] A second compound, $CH_3Re(O)_2(9,10-O_2C_6R_4)(NC_5H_5)$, was prepared by the oxidation of $MeReO_2$, obtained in-situ from MTO and polymer-supported PPh_3, with phenanthrenequinone.[24] In effect, the condensation reaction between Re(VII) and catechol ($CatH_2$, meant to include ring-substituted 1,2-dihydroxyarenes in general) affords one route to $MeReO_2(1,2-Cat)$.[24] Oxidation of Re(V) by quinones forms the same material.[24] The net reactions are:

$$MeReO_3 + CatH_2 \rightleftharpoons MeRe(O)_2(Cat) + H_2O \tag{3a}$$

$$MeReO_2 + Quin \rightleftharpoons MeRe(O)_2(Cat) \tag{3b}$$
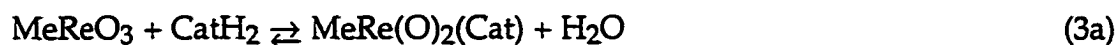
The products are best regarded as catecholate complexes of Re(VII). They are intensely colored species, shades of deep blue and violet depending on the substituents.[25] The spectroscopic characteristics undoubtedly arise from low-energy, allowed LMCT transitions. As indicated, these reactions are reversible. They proceed at measurable rates in aqueous and semi-aqueous media to extents that depend upon the identity of the catechol and particularly on the activity of water.[25]

To limit the number of variables we did not use MeReO$_2$ as the reagent, but instead chose related Re(V) compounds with a single oxorhenium group. We have thus studied the reactions of a series of mononuclear methyl(oxo)rhenium(V) compounds with quinones. In addition to the methyl and oxo groups, they contain a chelated dithiolate ligand, mtp or edt, and one other ligand, usually pyridine. They are rhenium(V) compounds, MeReO(mtp)Py (3) and MeReO(edt)Py (4), prepared by pyridine addition to dimer 1 (or 2) formed according to the equilibrium for reaction 4,

$$\{MeReO(dithiolate)\}_2 + 2\,Py \rightleftharpoons 2\,MeReO(dithiolate)Py \qquad K_1 \qquad (4)$$

The structural formulas of the participants are given in **Chart 1**. The structures of 1 and 3 have been established by single-crystal x-ray diffraction,[1] as has the PPh$_3$ analog of 4.[26] Upon reaction with quinone, pyridine is displaced in a reversible reaction,

$$MeRe^VO(dithiolate)Py + Q \rightleftharpoons MeRe^{VII}O(dithiolate)Cat + Py \qquad K_Q \qquad (5)$$

The thermodynamics and kinetics of these reactions have not been studied previously, neither for Re(VII) with catechol nor Re(V) with quinone. Two dithiolates were used in the course of this research, mtp and edt (Chart 1) and two quinones, phenanthrenequinone (PQ) and 3,5-di-*tert*-butylquinone (DBQ),

Chart 1. Structural formulas for participating compounds, with quinone and catechol shown generically
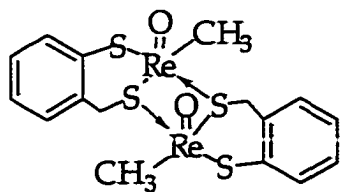
{MeReO(mtp)}$_2$ **1**
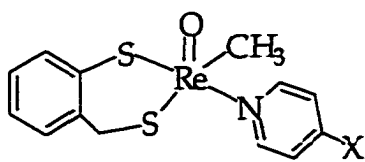
MeReO(mtp)NC$_5$H$_4$X **3**
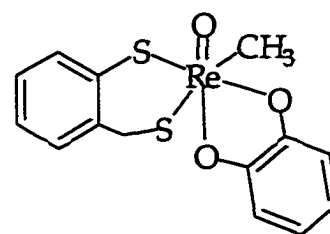
MeReO(mtp)Cat **5**
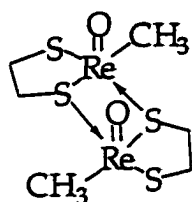
{MeReO(edt)}$_2$ **2**
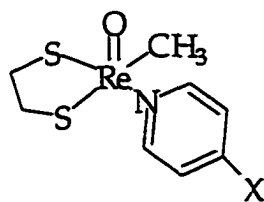
MeReO(edt)NC$_5$H$_4$X **4**
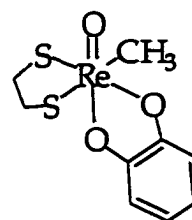
MeReO(edt)Cat **6**

PQ,
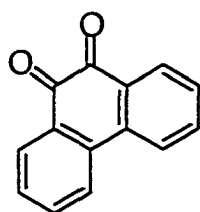
phenanthrenequinone
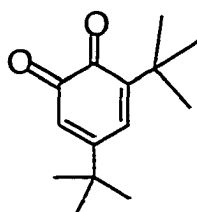
DBQ, 3,5-di-*tert*-butyl-1,2-

benzoquinone

each with one of five pyridine ligands. These reactions do not attain completion, but reach an equilibrium position dependent on the particular reagents used and their concentrations. The objectives of this research have been to characterize the kinetics, identify the steps that comprise the mechanism, and evaluate their rates and equilibrium constants.

Experimental Section

Materials. Benzene (Fisher spectranalyzed) was used as the solvent for all UV-Vis kinetic studies. The solvent utilized for NMR studies was deuterated benzene (Cambridge Isotope Laboratories). Dimer 1 was prepared as described in the literature[1] and dimer 2 was synthesized from $Me_2Re_2O_2(SPh)_4$, $edtH_2$ and dimethyl sulfide.[3] Pyridine (Fisher) was used as received. Other reagents, including 1,2-phenanthrenequinone, 3,5-di-tert-butylbenzoquinone, and ring-substituted pyridines were purchased from Aldrich and used as received.

Instrumentation. UV-Visible kinetic studies were carried out with the use of Shimadzu scanning spectrophotometers equipped with electronic temperature controlled cell holders. A Shimadzu diode-array spectrophotometer was used for rapid, repetitive spectral scans. ^1H NMR spectra were acquired with the use of Bruker DRX–400 or Varian VXR–400 spectrometers. The ^1H chemical shifts were referenced to the residual proton resonance of the deuterated benzene, $\delta = 7.16$ ppm.

Results

Equilibrium Constants. The equilibrium constants (K_1) for the monomerization reaction (eq 4) between $\{MeReO(mtp)\}_2$ and five ring-substituted pyridines are available in the literature[6] and are given in **Table 1.** The values of K_1 for the previously unexplored compound $\{MeReO(edt)\}_2$ were determined from the spectra of solutions of this dimer in equilibrium with each of five pyridines, generically designated Py. The program PSEQUAD[27] was used to determine K_1 by a global fit of absorbance-concentration data taken at 22 wavelengths in the range 400–620 nm. The concentrations were 0.8 mM Re_T and 0.5–41 mM Py. The values of K_1 so calculated are given in **Table 1.** The values of K_1 for the mtp and edt complexes do not differ greatly.

The reactions of MeReO(dithiolate)Py (or M–Py) complexes with quinones are accompanied by a large absorbance increases, signaling the formation of the intensely absorbing product MeReO(dithiolate)Cat. The equilibrium constants (K_Q) for those reactions were determined directly from the equilibrium absorbances. These experiments were carried out with $[PQ] \ll [M-Py]$. The equilibrium absorbance per cm of optical path is given by

$$\text{Abs} = \varepsilon_{M-Py}[M-Py] + \varepsilon_{M-Cat}\left(\frac{K_Q \dfrac{[M-Py]}{[Py]}}{1 + K_Q \dfrac{[M-Py]}{[Py]}}\right)[PQ]_T \tag{6}$$

Table 1. Equilibrium Constants for Monomerization $(K_I,$ eq 4) and Quinone/Catecholate $(K_Q,$ eq 5) Reactions

Pyridine	MeReO(mtp)-Py		MeReO(edt)-Py	
	$K_I/10^3 \, M^{-1}$ [a,b]	K_Q [c]	$K_I/10^3 \, M^{-1}$ [a]	K_Q [c]
$4\text{-Bu}^t C_5 H_4 N$	4.07	9.2(3)	3.16(7)	3.2(2)
$4\text{-MeC}_5 H_4 N$	1.00	12.0(5)	2.24(5)	3.5(2)
$3\text{-MeC}_5 H_4 N$	1.07	22.6(6)	1.26(3)	5.0(2)
$4\text{-PhC}_5 H_4 N$	1.15	21.7(6)	0.98(2)	5(1)
$C_5 H_5 N$	0.174	42.7(7)	0.25(1)	11.2(4)

[a]For reaction 4; [b]from Ref[7]; [c]for reaction 5

The values of the equilibrium constants, K_Q, determined by least-squares fitting are given in **Table 1**. The absorption maximum and molar absorptivity of each M–Cat species are summarized in **Table 2**. An example of that is given in the Supporting Information, **Figure S–1**. The reactions of DBQ proceeded to completion at all the concentrations used, allowing the spectrum of the product to be determined by direct measurement.

Kinetics. Spectrophotometric methods were used throughout, following the buildup of the product. A typical repetitive scan experiment is shown in **Figure 1**. These determinations were conducted principally at the absorption maximum with occasional checks at other wavelengths.

The kinetic data for the PQ reactions were analyzed by reversible kinetics, according to the rate equation

$$-\frac{d[M-Py]}{dt} = \frac{d[M-Cat]}{dt} = k_f[M-Py]\cdot[PQ] - k_r[M-PCat]\cdot[Py] \tag{7}$$

With [MeReO(mtp)Py] at concentrations much higher than those of the other species, the approach to equilibrium follows pseudo-first-order kinetics. The rate constant for equilibration is given by

$$k_e = k_f[M-Py] + k_r[Py] \tag{8}$$

Table 2. Visible and ^{1}H–NMR Spectra of MeRe^{VII}O(dithiolate)Cat^a and MeRe^V(dithiolate)Py Complexes

Compound	$\lambda_{max}(\epsilon/10^3$ L mol^{-1} cm$^{-1})$ ^{b}		^{1}H NMR, Re-CH$_3$ δ ^{c,d}	
	mtp	edt	mtp	edt
MeReO(dithiolate)Py	608 (0.255)	545 (0.234)	2.77(s)^e	2.46(s)
MeReO(dithiolate)PCat	595 (15.9)	581 (13.7)	1.85(s)	2.18(s)
MeReO(ditholate)DBCat	550 (17.0)	531 (10.7)	1.74, 1.77^f	2.47, 2.70^f

^{a}PQ = phenanthrenequinone; DBQ = 3,5-di-*tert*-butylquinone; ^{b}For PQ, from extrapolation of the spectrum to high [M-Py]; for DBQ, from the measured absorbances; ^{c}in C$_6$D$_6$; ^{d}The chemical shifts for the CH$_2$ groups of dithiolate ligands are: MeReO(mtp)PCat, δ 5.23 (d, 1H), 5.48 (d, 1H); MeReO(edt)PCat, 3.56 (m, 2H), 4.08 (m, 1H), 4.18 (m, 1H); MeReO(edt)Py 2.76 (br, 2H), 3.25 (br, 1H), 4.01 (br, 1H); MeReO(mtp)DBCat (two isomers) 5.06 (d, 1H), 5.19 (d, 1H), 5.44 (m, 2H); MeReO(edt)DBCat (two isomers), 3.22 (m, 2H) 3.66 (m, 2H), 3.83 (m, 2H), 4.17 (m, 1H), 4.28 (m, 1H); ^{e}Ref. ^{7}; ^{f}Two isomers are present; see text.
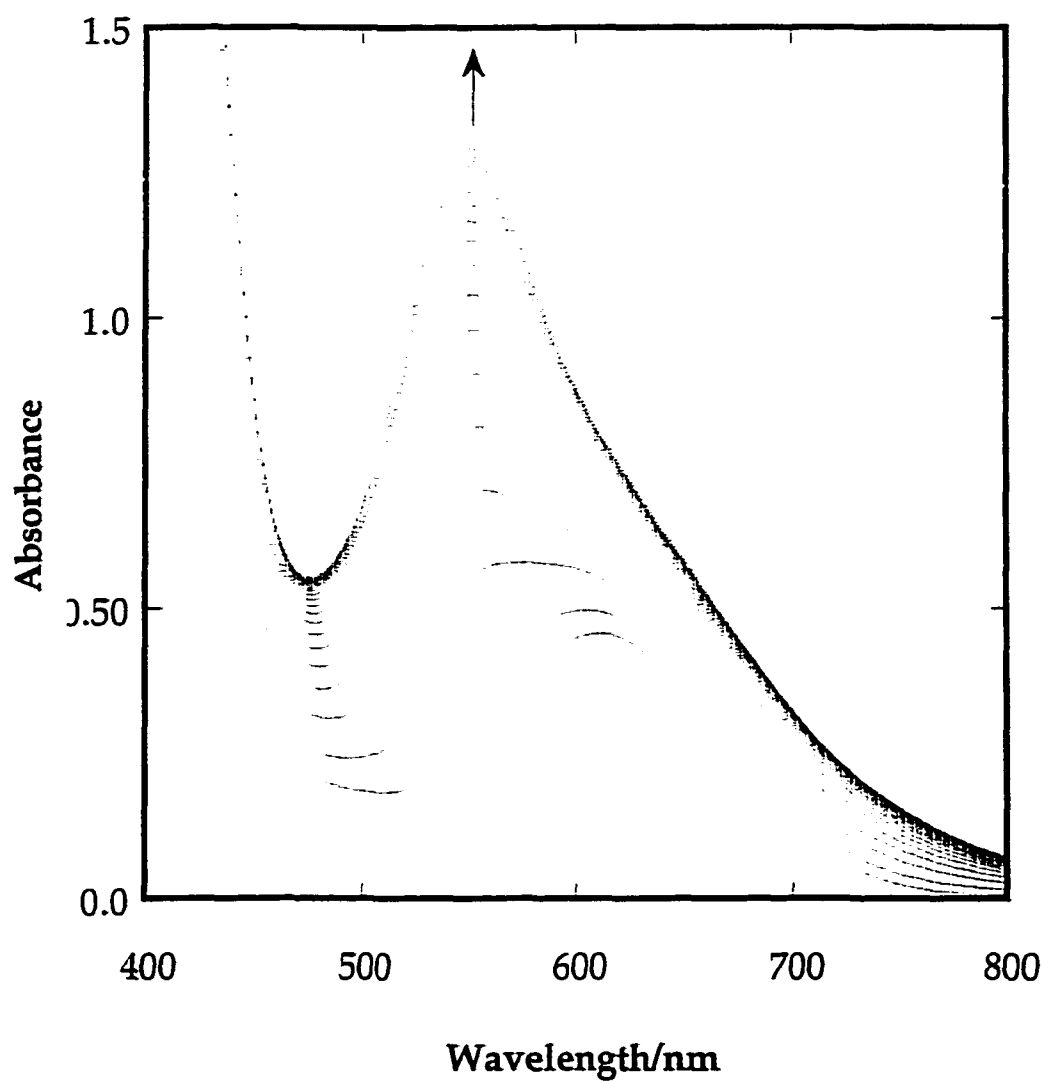
Figure 1. Repetitive scans in a 1-cm cuvette of the visible spectrum during a reaction between 2.0 mM MeReO(mtp)Py and 60 μM DBQ in the presence of 18 mM Py in benzene at 25.0 °C. The interval between scans was 12 s, except for the first two spectra, where it was 5.

One method of exploring the fit to this equation is provided by this rearranged equation,

$$\frac{k_e}{[Py]} = k_r + k_f \frac{[M-Py]}{[Py]} \tag{9}$$

Figure 2 displays the data for MeReO(mtp)Py and MeReO(edt)Py against the indicated concentration ratio. The data are indeed linear, confirming this model. The intercept affords k_r from the intercept and k_f from the slope. Values of the rate constants that are more meaningful statistically can be obtained by direct fits to eq 7 using a program that accommodates two x-variables.[28] The rate constants obtained by the latter method are given in Table 3. The kinetic data for the DBQ reactions, which proceeded to completion, were fit to first-order kinetics. The values of the pseudo-first-order rate constants (k_ψ) were determined as a function of [MeReO(mtp)Py], the concentration of which was chosen to be >> [DBQ]. As shown in Figure S–2 in the Supporting Information, k_ψ varies linearly with [MeReO(mtp)Py] and the line extrapolates to the origin. These rate constants are $k_5 = 4.02(5)$ L mol^{-1} s^{-1} for 4-Bu^{t}C$_5$H$_5$N and 8.4(1) L mol^{-1} s^{-1} for C$_5$H$_5$N.

We attempted to shift the equilibrium position of M-DBCat systems back to the left (eq 5) by diluting with solvent simultaneously with all the components other than Py, in order to evaluate the equilibrium constant and the reverse rate constant more directly. This was not successful, as the decomposition of MeReO(mtp)DBCat interfered. Insofar as we could determine, the reaction of DBQ proceeds entirely to completion.
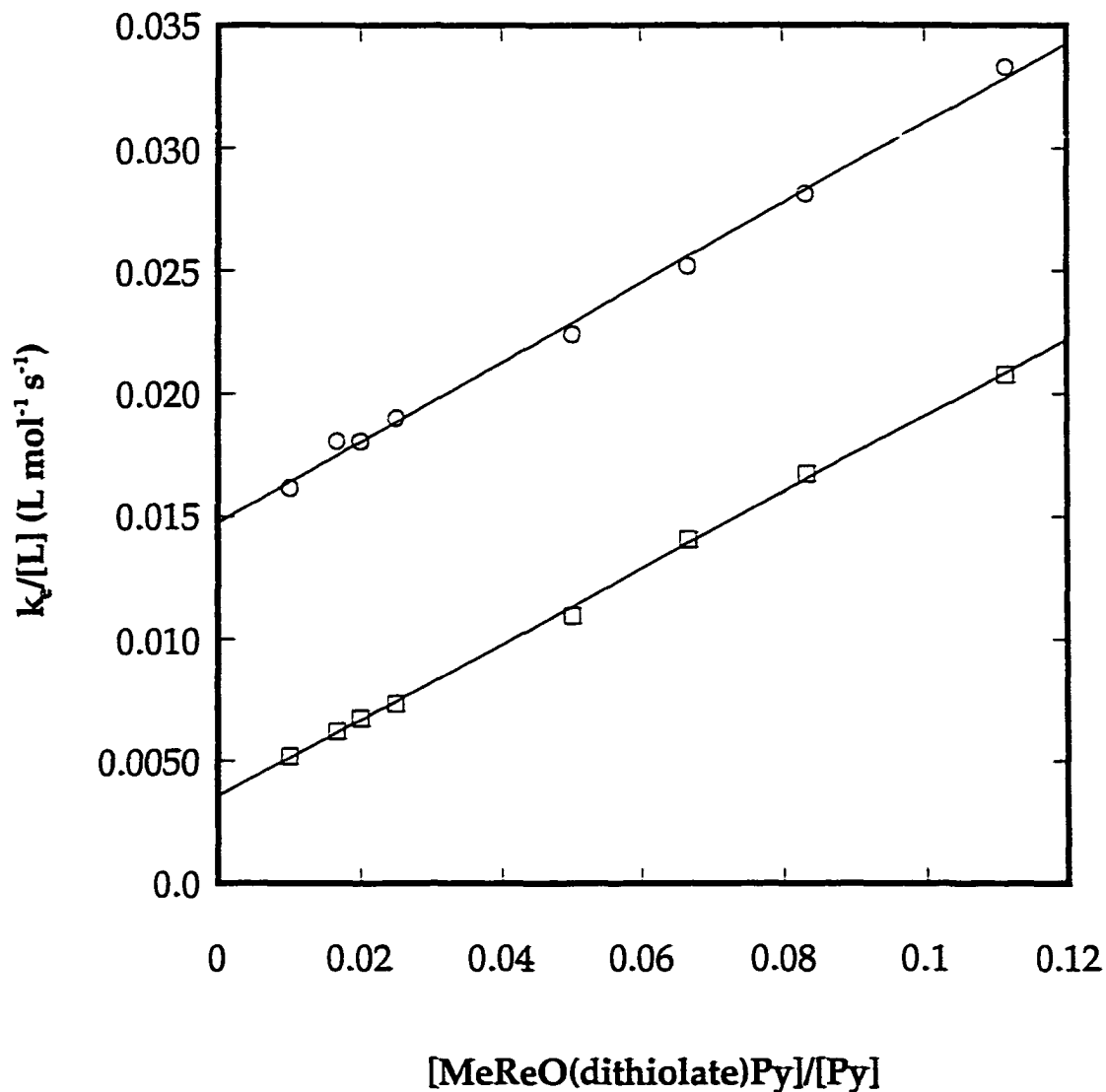
Figure 2. Analysis of the kinetic data for the equilibration kinetics for the reactions of MeReO(dithiolate)Py with PQ, by plots of k_e/[Py] against [MeReO(dithiolate)Py]/[Py] according to eq 9. Values are shown for dithiolate = mtp (squares) and edt (circles) pertaining to experiments in benzene at 25.0 °C.

Table 3. Rate Constants for the Forward and Reverse Steps of the Reactions Between MeReO(dithiolate)–Pyridine and Phenanthrenequinone[a]

Pyridine	$k_f/10^{-2}$ L mol^{-1} s^{-1}		$k_r/10^{-3}$ L mol^{-1} s^{-1}	
	mtp	edt	mtp	edt
4-Bu^{t}C$_5$H$_4$N	5.3(1)	6.6(4)	5.71(6)	20.6(2)
4-MeC$_5$H$_4$H	6.5(2)	7.7(5)	5.4(1)	22.0(2)
3-MeC$_5$H$_4$N	9.1(2)	7.7(2)	4.01(6)	15.4(1)
4-PhC$_5$H$_4$N	9.4(2)	11(3)	4.36(6)	21(1)
C$_5$H$_5$N	15.5(1)	16.4(5)	3.63(5)	14.7(2)

[a]In benzene at 25.0 °C.

The ^{1}H NMR spectra for the complexes derived from 3,5-di-*tert*-butyl-1,2-benzoquinone, which are presented in **Table 2**, indicate the presence of two stereoisomers:

as shown for edt, and likewise for mtp. There is little difference between them, and it is not surprising that the two are formed in nearly the same amount. This means that the rate constant is the sum of two nearly identical rate constants for each isomer.

Activation Parameters. Rate constants for the forward and reverse directions of reaction 5 with "Py" = 4-Bu^{t}C$_5$H$_4$N and "dithiolate" = mtp were evaluated as a function of temperature over the range 288–333 K. The data were analyzed according to the transition state theory equation,

$$\frac{k}{T} = \frac{k_B}{h} \cdot e^{(\Delta S^{\ddagger}/R)} \cdot e^{(-\Delta H^{\ddagger}/RT)} \tag{10}$$

The activation parameters are:

	$\Delta H^{\ddagger}$ / kJ mol^{-1}	$\Delta S^{\ddagger}$ / J K^{-1} mol^{-1}
MeReO(mtp)NC$_5$H$_4$-4-Bu^t + PQ	53(2)	−92(6)
MeReO(mtp)PCat + 4-Bu^{t}C$_5$H$_4$N	62(3)	−82(6)

Reactions of the Re Dimers with Quinones. A reaction occurred between {MeReO(mtp)}$_2$ and PQ, as evidenced by the very slow increase in absorbance at 595 nm, consistent with the formation of MeReO(mtp)PCat. This occurred quite slowly in comparison with reaction 5. The same reaction was then explored by adding 60 μM pyridine to the other two reagents. This led to a considerable increase in the rate of product formation, as shown in **Figure S–3**. This effect of Py can be attributed to the occurrence of reactions 4 and 5 in succession.

Reactions of Phosphines. Two types of experiments were carried out. In the first, MeReO(mtp)PPh$_3$ and an ortho-quinone (in this case, 1,2-napthoquinone) were mixed. No rhenium catecholate was observed. It is known that the values of K_1 for phosphine ligands are much larger than those for pyridines, so much so that K_1 values could not be determined for phosphines.[6] Further, the values of the equilibrium constants K_Q for quinone reactions are not large numbers, **Table 1**. These two facts combine to indicate that it is not at all surprising to find that no reaction occurred between the phosphine complex and the quinone.

A second experiment involved the attempt to react the first-formed catecholate, MeReO(mtp)PCat with triphenylphosphine, reasoning that the strongly-coordinating phosphine should release free quinone:

$$MeReO(mtp)PCat + PPh_3 \rightarrow PQ + MeReO(mtp)(PPh_3) \qquad (11)$$

The spectrum of the rhenium catecholate complex was indeed slowly bleached after phosphine was added. This bleaching could be the result of two different independent or simultaneous reactions. One is that shown in eq 11, the other is that between PPh_3 and M–Py. This situation proved to be quite complex, and not informative as to the matter being explored; it was not pursued further.

Other diones. Mixing $MeReO(mtp)NC_5H_4Me^m$ with 2-methyl-1,4-napthoquinone gave no evidence of formation of a rhenium complex. This is not surprising because a chelating catecholate cannot form; it does establish, however, that simple coordination is not a proper description of the reactions of the ortho-quinones.

Along the same line, an experiment was carried out with 1,2-cyclohexanedione and MeReO(mtp)Py in C_6D_6. The green color of the parent compound remained unchanged, as did its NMR spectrum even after two days.

Discussion

Spectra of MeReO(dithiolate)Py and MeReO(dithiolate)Cat Complexes. The visible spectra (Table 2) of all M-Py complexes exhibit a d-d band at 545 (edt) and 608 (mtp) nm, with respective molar absorptivities 234-255 $L\ mol^{-1}\ cm^{-1}$. The band lies at a higher energy for MeReO(edt)Py as compared to MeReO(mtp)Py

because the edt ligand is more electron-donating than mtp. The MeReO(dithiolate)Cat complexes exhibit absorption maxima in the same wavelength region, but the molar absorptivities are nearly two orders of magnitude larger. Their intensity indicates that they are LMCT bands, arising from the donation of ligand electron density into the d orbitals of the metal.

Equilibrium Constant of Monomerization Reactions. The values of K_1 (Table 1) for the reaction in which {MeReO(dithiolate)}$_2$ reacts with a pyridine ligand decrease as the electron-donating ability of that ligand decreases. From the present work, the range of the K_1 values for the edt complex is 0.25×10^3 (Py) to 3.2×10^3 (4-Bu^{t}C$_5$H$_4$). This study was limited to pyridine and those of its derivatives that are stronger Lewis bases, to avoid the intrusion of the parent dimer into the reaction of M-Py complexes with quinones.

Equilibrium Constant of Quinone Reactions. The reaction referred to is written in eq 5 and its equilibrium constant is designated as K_Q. The values of K_Q are > 1, with a magnitude that increases as the Py ligand becomes less electron-donating. For example, for MeReO(edt)Py, the values of KQ range from 3.2 (4-Bu^{t}C$_5$H$_4$) to 11.2 (C$_5$H$_5$N). These values, and the trend they display, reflect the rate constants for the forward and reverse directions, as presented subsequently.

Comparison of K_1 and K_Q. There is a thermodynamically-specified relation between the values of K_1 and K_Q. They are related by the chemical equation obtained by adding one-half of eq 4 to eq 5:

$$1/2 \ \{MeReO(dithiolate)\}_2 + Q \rightleftarrows MeReO(dithiolate)Cat \qquad K_c \qquad (12)$$

The relationship between the three equilibrium constants is thus

$$K_C = \frac{1}{2}K_I \times K_Q \tag{13}$$

which can also be written

$$\log K_Q = \log K_C - \frac{1}{2}\log K_I \tag{14}$$

The internal consistency of these data have been confimed, and thus the model validated, by the linear plot of $\log K_Q$ against $\log K_I$ presented **Figure 3**, with a slope of –0.5 and an intercept that affords the value of $\log K_C$.

Kinetics of the Reaction of MeReO(dithiolate)Py with PQ. As the pyridine becomes a weaker Lewis base, the forward rate constant increases by a factor of about three whereas the reverse rate constant decreases only slightly, see **Table 3**. The forward rate constant, for PQ addition, varies mildly among the Py ligands being displaced. (1) all variations are mild: a factor of about 3 encompasses the value. (2) the most weakly-held pyridine is the one most readily displaced by PQ.

Comparisons between mtp and edt Complexes. The rate constants for the reactions of PQ with MeReO(mtp)Py and MeReO(edt)Py, for a given pyridine, are roughly the same. In the reverse direction, however, the edt complex is about four times more reactive. Thus the reverse reaction depends on the characteristics of the ancillary dithiolate ligand. The edt is the more electron-donating of the two; it therefore releases the catechelato-oxygen more readily, allowing the pyridine to reenter.

Kinetics of the Reaction between MeReO(mtp)Py and DBQ. This reaction proceeds to completion, and the reverse rate constant cannot be determined.
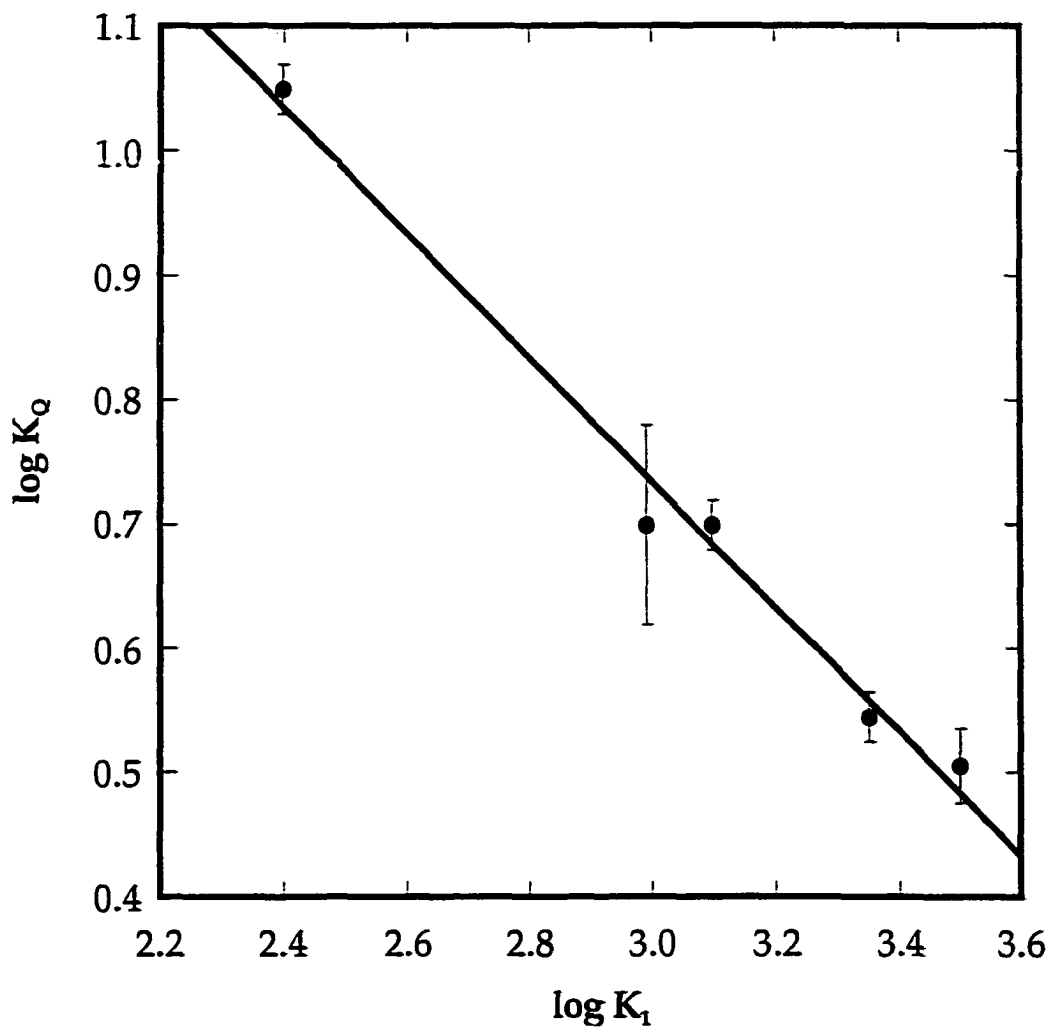
Figure 3. Comparison of the equilibrium constant of monomerization of $\{MeReO(edt)\}_2$, K_1, with the equilibrium constant of MeReO(edt)PCat formation, K_Q. As thermodynamics dictate, the slope is -0.50 ± 0.04.

Moreover, the forward rate constant is 50-fold greater than that for PQ, consistent with DBQ being much more electron-donating. Clearly, the forward rate constant depends strongly on the characteristics of the entering ligand.

Activation Parameters. The negative values of $\Delta S^{\ddagger}$ are probably reflective of little more than these being second-order reactions in which the diffusion and orientation of the pair of solute molecules dominates. We later propose the intervention of a reaction intermediate whose formation requires substantial organization. Indeed, the entropic barrier is substantial, $T\Delta S^{\ddagger}$ being roughly 26 kJ, about half the barrier from $\Delta H^{\ddagger}$.

Proposed Mechanism. The experimental data show effects of entering PQ and DBQ, which are quite substantial. The rate constant is larger for DBQ by a factor of 76 (4-Bu^{t}C$_5$H$_4$N) or 54 (C$_5$H$_5$N). For a given quinone, the effect of the change from 4-Bu^{t}C$_5$H$_4$N to C$_5$H$_5$N is minimal: a factor of 2.1 (DBQ) to 2.9 (PQ). These trends signal an associative mechanism, with major involvement of Re–O bond-making in the transition state and relatively little Re–Py bond breaking. The reaction can be described as shown in **Scheme 1**. In the first step, the quinone approaches the vacant coordination site on the Re(V) reagent, interacting weakly with it. This generates an intermediate in which there is weak coordination of the quinone. The suggestion of a six-coordinate rhenium intermediate is supported by the recent preparation of such a complex, MeReO(edt)(2,2′-bpy).[29] This intermediate undergoes a turnstile rotation,[30-34]

placing the Py ligand *trans* to the oxo group. The turnstile mechanism has been proposed to explain the kinetics of monodentate ligand substitution reactions of these Re(V) complexes.[35] The *trans*-influence of the oxo ligand causes the Re-Py bond to elongate and then break. Finally, internal electron transfer and ring-closure take place giving rise to the Re(VII)–catecholate product. In the reverse direction the identity of the ancillary dithiolato ligand exhibits a small effect on the rate constant, while there is an even smaller effect of the identity of the entering pyridine ligand. The reverse reaction requires de-chelation of the catecholate in order for Py to attack. The more electron density on the Re (edt vs mtp) the faster the de-chelation. This step must be very slow when the leaving group is DBQ because the reverse rate constant cannot be measured. We propose that the first reaction is an equilibrium that is established much more rapidly than the rate-controlling steps. The combination of the turnstile rotation, Re–Py bond breaking/making and internal electronic transformations are thus rate-controlling in both directions.

Scheme 1
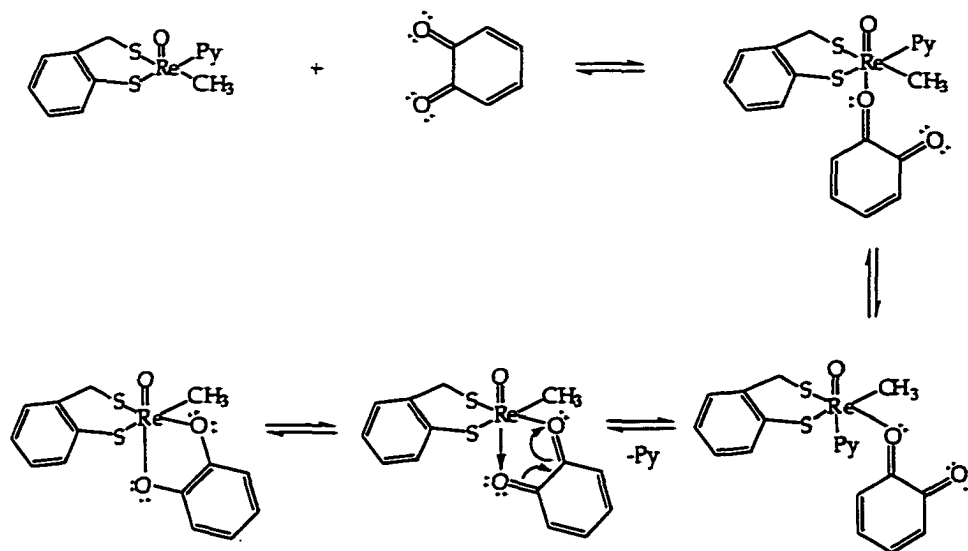
Comments on Structure. The reaction product is, to our knowledge, the first example of a rhenium(VII) dithiolate complex that does not immediately release the organic disulfide by internal electron transfer. For example, the Re(VII) compounds MeRe(O)$_2$(mtp)OPy, unless intercepted by a second phosphine reagent, undergoes reversible decomposition:[5,36]
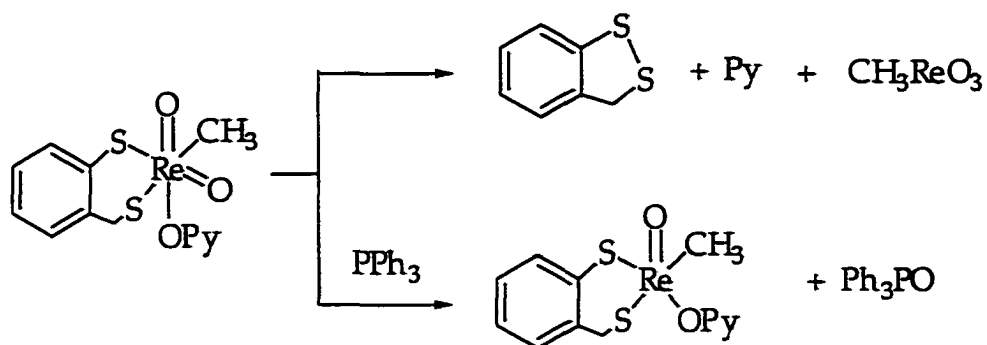
Our assignment of MeReO(dithiolate)Cat complexes as being catecholates in fact follows from results presented by other investigators. The Re(VII) catecholate complexes that have been previously reported are all intensely colored blue and

purple compounds.[24,25] The crystal structures define the C–O bond lengths indicative of a catechol (133.7–138.7 pm) as opposed to a semiquinone (127.2–131.2 pm).[37] As of yet, all complexes of rhenium in high oxidation states with quinone-based ligands exist as catecholate complexes in the solid state.[16-18,20-22,24,37] Catecholates can donate more π-electron density than semiquinones and are therefore favored by metals in a high oxidation state. Pierpont suggests that the charge distribution in such compounds is related to the energies of the quinone π-orbitals and the metal d-orbitals.[37] The charge will reside in the orbitals of lower energy, in this case the metal quinone orbitals, giving rise to metal-catecholate compounds.

Other Considerations. This is the first case in which "stable" Re(VII)-dithiolate compounds have been obtained. Even so, the complexes do not persist indefinitely. The dithiolate ligand does slowly become oxidized to the disulfide, $MeReO_3$ being formed concurrently. The formation of metal-oxo bonds is an additional driving force. Our data suggest that quinones may be able to trap Re(V) intermediates.

The condensation of catechols with Re(VII) and the oxidation of Re(V) by quinones bear a conceptual relation to the respective reactions with H_2O_2 and O_2. The condensation reaction between $MeReO_3$ and hydrogen peroxide forms a cyclic peroxide.[38-41] Also, $MeReO_2$ reacts with O_2 to give the same product, albeit with complications from the phosphine.[42]

$$\underset{\substack{Me}}{\overset{O}{\underset{\|}{Re}}}\!\!=\!\!O \quad \xrightarrow[-H_2O]{H_2O_2} \quad O\!\!=\!\!\underset{Me}{\overset{O}{\underset{\|}{Re}}}\!\!<\!\!\overset{O}{\underset{O}{|}} \quad \xleftarrow{O_2} \quad MeReO_2(PPh_3)_2 \qquad (15)$$
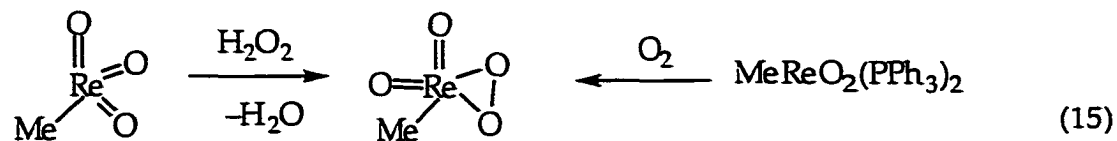
Acknowledgment.

This research was supported by the U. S. Department of Energy, Office of Basic Energy Sciences, Division of Chemical Sciences under contract W-7405-Eng-82.

Supporting Information Available.

Figures and tables showing the electronic spectra, the analysis of kinetic data, and time-course data for reactions of MeReO(dithiolate)Py with phenanthrenequinone (9 pages). This material is available gratis at http://pubs.acs.org.
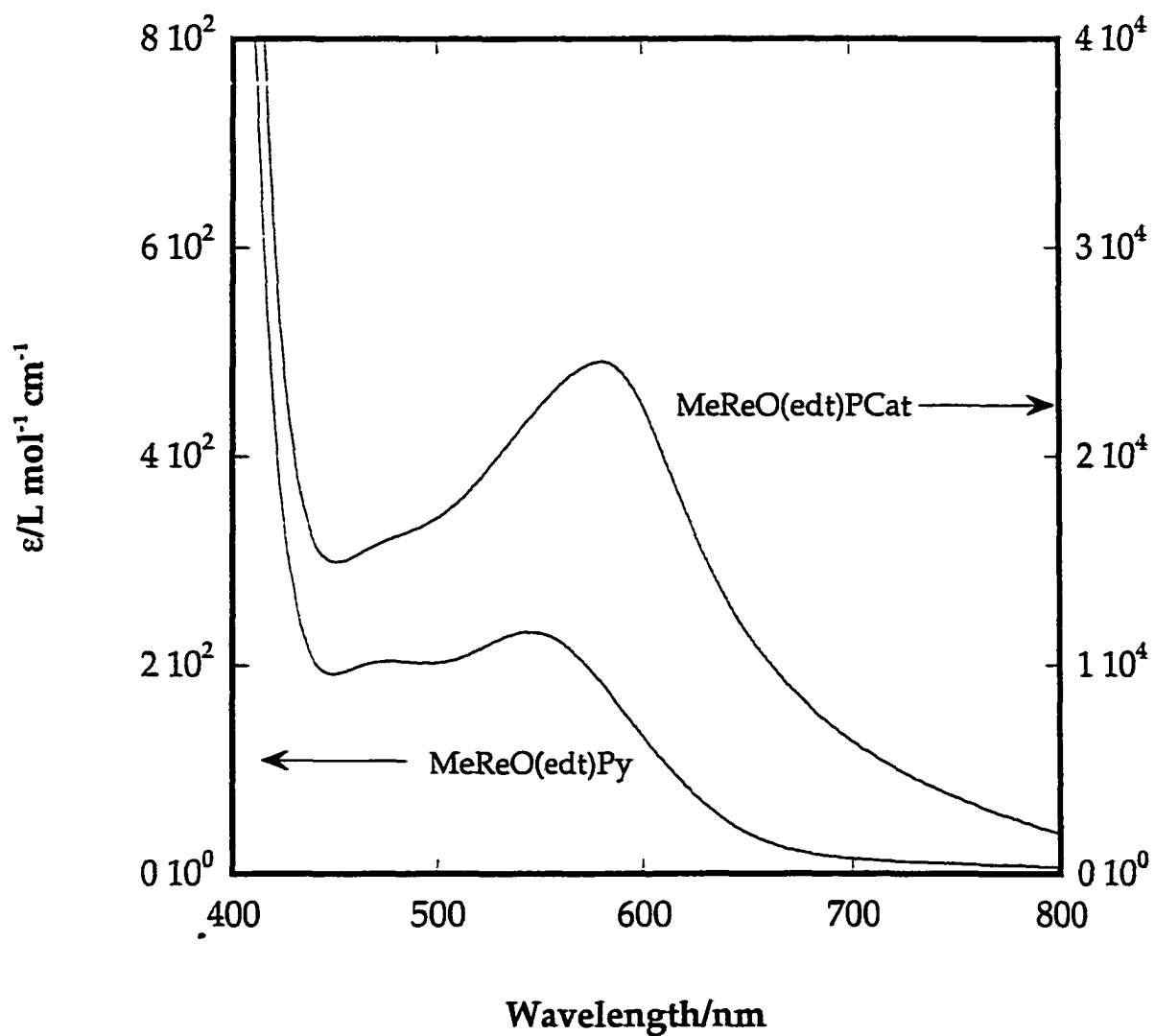
Figure S-1. UV-Visible Spectra of MeReO(edt)Py (2 mM) and a MeReO(edt)PCat (33 μM).
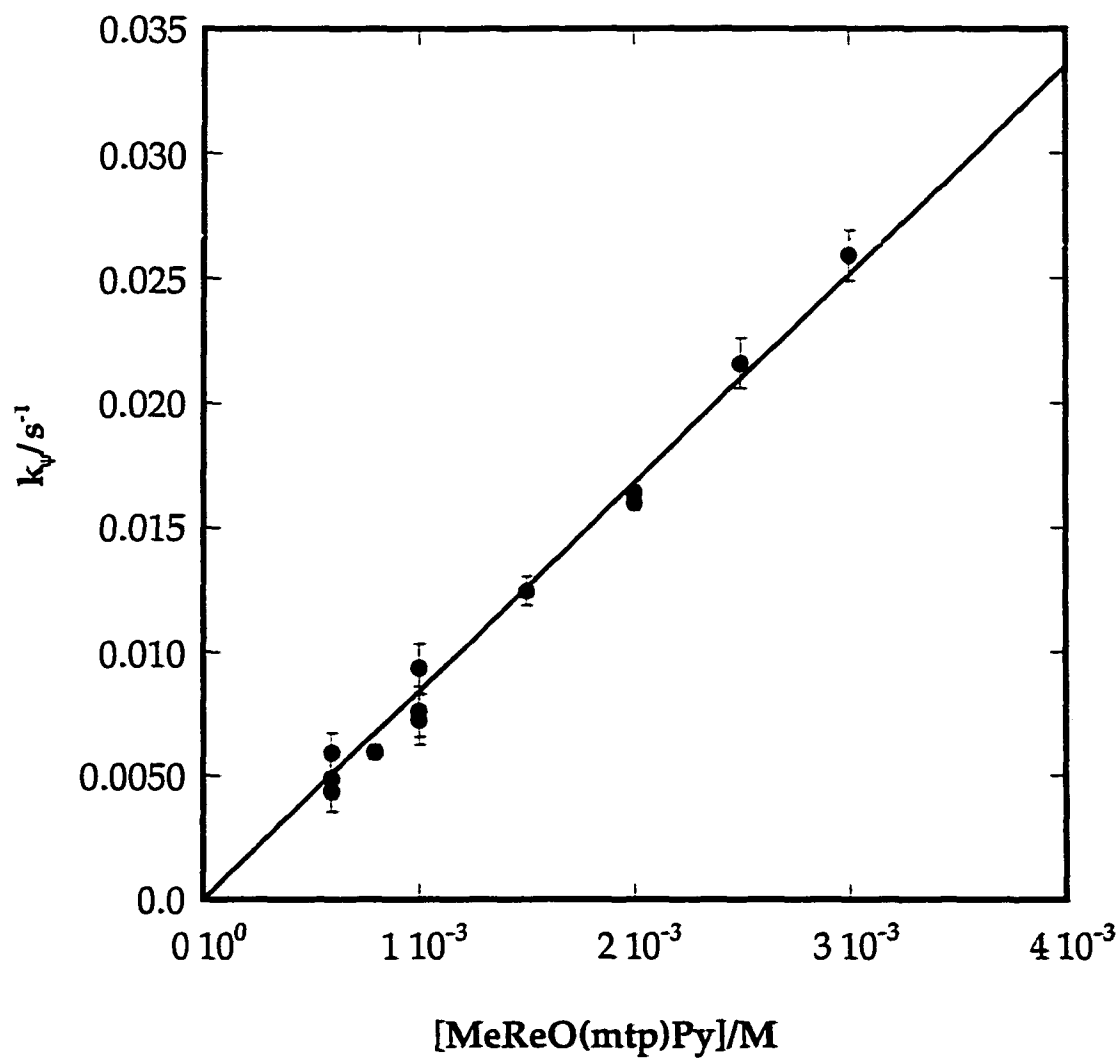
Figure S-2. Analysis of the kinetic data for the reaction of MeReO(mtp)Py with DBQ in benzene at 25 °C. The second order rate constant is $k_5 = 8.4(1)$ L mol^{-1} s^{-1}.
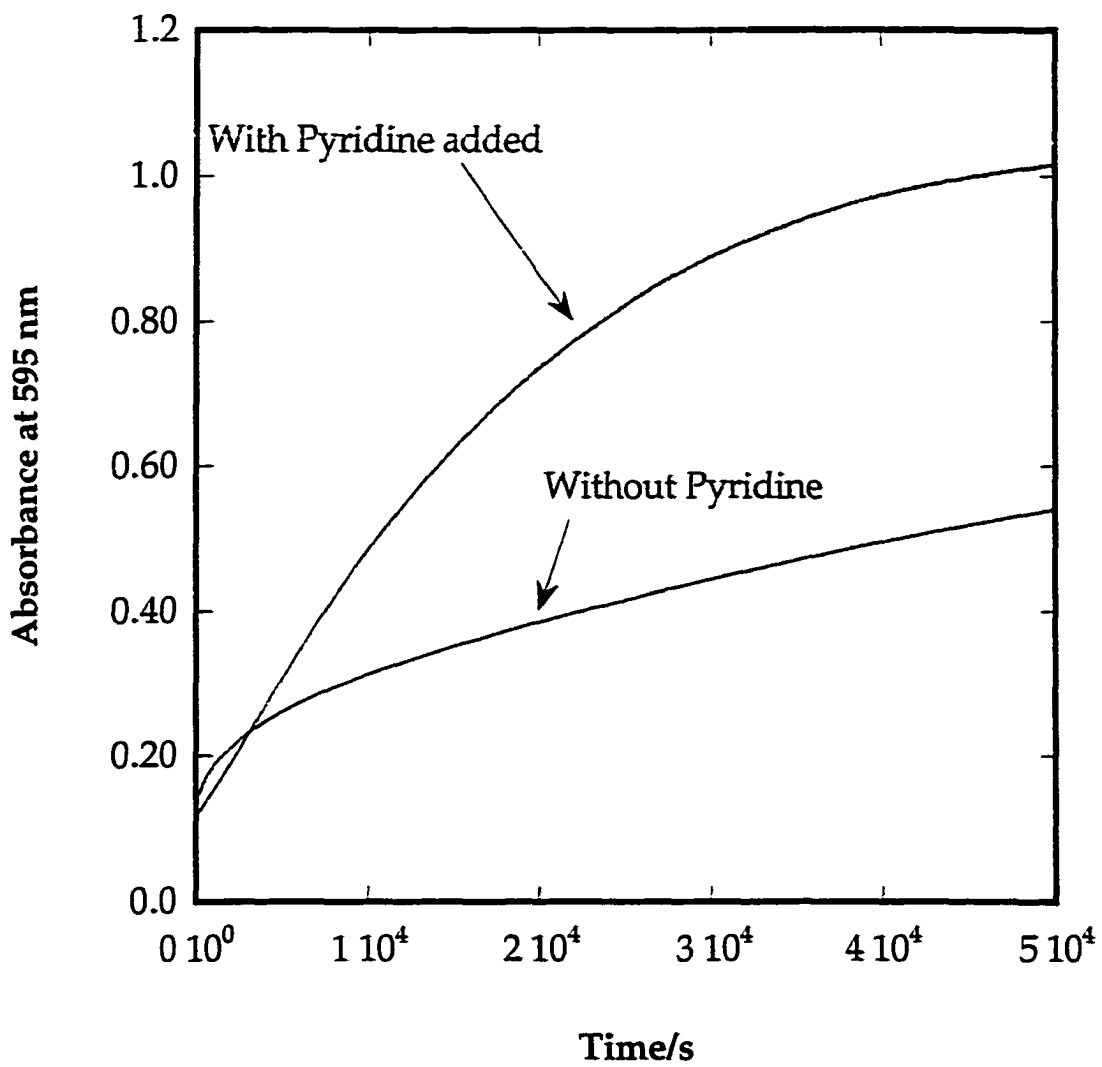
Figure S-3. UV-Visible time courses of the reaction (mtp)D (2 mM) with phenanthrenequinone (60 μM) both in the absence and presence (60 μM) of pyridine at 25.0 °C.

Table S-1: Data for the reaction of PQ and MeReO(edt)L, where L = 3-picoline

[MeReO(edt)L]/M	[L]/M	[PQ]/M	k_e/s^{-1}	$Abs_{M\text{-}Cat}/cm^{-1}$
3.0×10^{-3}	1.2×10^{-2}	3.0×10^{-5}	4.21×10^{-4}	4.47×10^{-1}
2.0×10^{-3}	2.0×10^{-2}	3.0×10^{-5}	4.65×10^{-4}	2.61×10^{-1}
2.0×10^{-3}	3.0×10^{-2}	3.0×10^{-5}	6.06×10^{-4}	1.89×10^{-1}
1.0×10^{-3}	2.0×10^{-2}	3.0×10^{-5}	3.69×10^{-4}	1.49×10^{-1}
1.0×10^{-3}	4.0×10^{-2}	3.0×10^{-5}	6.82×10^{-4}	8.16×10^{-2}
1.0×10^{-3}	5.0×10^{-2}	3.0×10^{-5}	8.54×10^{-4}	6.45×10^{-2}
6.0×10^{-4}	3.6×10^{-2}	3.0×10^{-5}	6.07×10^{-4}	5.38×10^{-2}
6.0×10^{-4}	6.0×10^{-2}	3.0×10^{-5}	9.71×10^{-4}	3.06×10^{-2}

Table S-2: Data for the reaction of PQ and MeReO(edt)L, where L = 4-*tert*-butylpyridine

[MeReO(edt)L]/M	[L]/M	[PQ]/M	k_e/s^{-1}	Abs_{M-Cat}/cm^{-1}
2.0×10^{-3}	8.0×10^{-3}	3.0×10^{-5}	2.80×10^{-4}	3.37×10^{-1}
2.0×10^{-3}	1.2×10^{-2}	3.0×10^{-5}	3.98×10^{-4}	2.60×10^{-1}
2.0×10^{-3}	2.0×10^{-2}	3.0×10^{-5}	5.39×10^{-4}	1.81×10^{-1}
1.0×10^{-3}	1.5×10^{-2}	3.0×10^{-5}	3.81×10^{-4}	1.30×10^{-1}
1.0×10^{-3}	2.0×10^{-2}	3.0×10^{-5}	4.74×10^{-4}	1.00×10^{-1}
1.0×10^{-3}	4.0×10^{-2}	3.0×10^{-5}	9.02×10^{-4}	5.14×10^{-2}
6.0×10^{-4}	3.0×10^{-2}	3.0×10^{-5}	5.73×10^{-4}	4.39×10^{-2}
6.0×10^{-4}	3.6×10^{-2}	3.0×10^{-5}	7.69×10^{-4}	3.74×10^{-2}
6.0×10^{-4}	6.0×10^{-2}	3.0×10^{-5}	1.27×10^{-3}	2.05×10^{-2}

Table S-3: Data for the reaction of PQ and MeReO(edt)L, where L = 4-phenylpyridine

[MeReO(edt)L]/M	[L]/M	[PQ]/M	k_e/s^{-1}	Abs_{M-Cat}/cm^{-1}
3.0×10^{-3}	1.2×10^{-2}	3.0×10^{-5}	5.74×10^{-4}	4.35×10^{-1}
2.0×10^{-3}	1.2×10^{-2}	3.0×10^{-5}	4.86×10^{-4}	3.60×10^{-1}
1.0×10^{-3}	1.0×10^{-2}	3.0×10^{-5}	3.23×10^{-4}	2.54×10^{-1}
6.0×10^{-4}	9.0×10^{-3}	3.0×10^{-5}	2.67×10^{-4}	1.87×10^{-1}
3.0×10^{-3}	5.7×10^{-2}	3.0×10^{-5}	1.36×10^{-3}	1.65×10^{-1}
2.0×10^{-3}	8.0×10^{-2}	3.0×10^{-5}	2.10×10^{-3}	5.96×10^{-2}
1.0×10^{-3}	5.0×10^{-2}	3.0×10^{-5}	1.04×10^{-3}	6.97×10^{-2}
6.0×10^{-4}	3.6×10^{-2}	3.0×10^{-5}	7.35×10^{-4}	5.63×10^{-2}
6.0×10^{-4}	6.9×10^{-2}	3.0×10^{-5}	1.42×10^{-3}	2.73×10^{-2}

Table S-4: Data for the reaction of PQ and MeReO(edt)L, where L = 4-picoline

[MeReO(edt)L]/M	[L]/M	[PQ]/M	k_ψ/s^{-1}	Abs_{M-Cat}/cm^{-1}
3.0×10^{-3}	1.2×10^{-2}	3.0×10^{-5}	5.16×10^{-4}	3.90×10^{-1}
2.0×10^{-3}	2.0×10^{-2}	3.0×10^{-5}	5.91×10^{-4}	2.13×10^{-1}
2.0×10^{-3}	3.0×10^{-2}	3.0×10^{-5}	7.81×10^{-4}	1.55×10^{-1}
1.0×10^{-3}	2.0×10^{-2}	3.0×10^{-5}	5.05×10^{-4}	1.18×10^{-1}
1.0×10^{-3}	4.0×10^{-2}	3.0×10^{-5}	9.64×10^{-4}	5.91×10^{-2}
1.0×10^{-3}	5.0×10^{-2}	3.0×10^{-5}	1.18×10^{-3}	4.79×10^{-2}
6.0×10^{-4}	3.6×10^{-2}	3.0×10^{-5}	8.37×10^{-4}	4.17×10^{-2}
6.0×10^{-4}	6.0×10^{-2}	3.0×10^{-5}	1.37×10^{-3}	2.29×10^{-2}

Table S-5: Data for the reaction of PQ and MeReO(edt)L, where L = pyridine

[MeReO(edt)L]/M	[L]/M	[PQ]/M	k_e/s^{-1}	$Abs_{M\text{-}Cat}/cm^{-1}$
2.0×10^{-3}	1.8×10^{-2}	3.0×10^{-5}	5.99×10^{-4}	4.59×10^{-1}
2.0×10^{-3}	2.4×10^{-2}	3.0×10^{-5}	6.76×10^{-4}	N/A
1.0×10^{-3}	1.5×10^{-2}	3.0×10^{-5}	3.78×10^{-4}	3.50×10^{-1}
1.0×10^{-3}	2.0×10^{-2}	3.0×10^{-5}	4.49×10^{-4}	2.93×10^{-1}
1.0×10^{-3}	4.0×10^{-2}	3.0×10^{-5}	7.60×10^{-4}	1.81×10^{-1}
6.0×10^{-4}	3.0×10^{-2}	3.0×10^{-5}	5.41×10^{-4}	1.53×10^{-1}
6.0×10^{-4}	3.6×10^{-2}	3.0×10^{-5}	6.50×10^{-4}	1.31×10^{-1}
6.0×10^{-4}	6.0×10^{-2}	3.0×10^{-5}	9.69×10^{-4}	8.23×10^{-2}

Table S-6: Data for the reaction of PQ and MeReO(mtp)L, where L = 3-picoline

[MeReO(mtp)L]/M	[L]/M	[PQ]/M	k_e/s^{-1}	Abs_{M-Cat}/cm^{-1}
9.0×10^{-3}	3.6×10^{-2}	3.0×10^{-5}	9.92×10^{-4}	4.03×10^{-1}
6.0×10^{-3}	3.0×10^{-2}	3.0×10^{-5}	6.62×10^{-4}	3.86×10^{-1}
6.0×10^{-3}	4.0×10^{-2}	3.0×10^{-5}	7.08×10^{-4}	3.74×10^{-1}
3.0×10^{-3}	3.0×10^{-2}	3.0×10^{-5}	3.62×10^{-4}	3.25×10^{-1}
3.0×10^{-3}	4.5×10^{-2}	3.0×10^{-5}	4.38×10^{-4}	2.72×10^{-1}
3.0×10^{-3}	6.0×10^{-2}	3.0×10^{-5}	5.00×10^{-4}	2.37×10^{-1}
3.0×10^{-3}	9.0×10^{-2}	3.0×10^{-5}	6.05×10^{-4}	2.14×10^{-1}
3.0×10^{-3}	1.5×10^{-1}	3.0×10^{-5}	8.60×10^{-4}	1.39×10^{-1}
3.0×10^{-3}	2.2×10^{-1}	3.0×10^{-5}	1.15×10^{-3}	1.02×10^{-1}
3.0×10^{-3}	3.0×10^{-1}	3.0×10^{-5}	1.50×10^{-3}	7.09×10^{-2}

Table S-7: Data for the reaction of PQ and MeReO(mtp)L, where L = 4-*tert*-butylpyridine

[MeReO(mtp)L]/M	[L]/M	[PQ]/M	k_e/s^{-1}	Abs_{M-Cat}/cm^{-1}
9.0×10^{-3}	3.6×10^{-2}	3.0×10^{-5}	6.75×10^{-4}	3.27×10^{-1}
6.0×10^{-3}	3.0×10^{-2}	3.0×10^{-5}	4.80×10^{-4}	2.93×10^{-1}
6.0×10^{-3}	4.0×10^{-2}	3.0×10^{-5}	5.53×10^{-4}	2.76×10^{-1}
3.0×10^{-3}	3.0×10^{-2}	3.0×10^{-5}	3.57×10^{-4}	2.29×10^{-1}
3.0×10^{-3}	4.5×10^{-2}	3.0×10^{-5}	4.04×10^{-4}	1.82×10^{-1}
3.0×10^{-3}	9.0×10^{-2}	3.0×10^{-5}	6.48×10^{-4}	1.15×10^{-1}
3.0×10^{-3}	1.5×10^{-1}	3.0×10^{-5}	1.03×10^{-3}	7.43×10^{-2}
3.0×10^{-3}	3.0×10^{-1}	3.0×10^{-5}	1.87×10^{-3}	3.85×10^{-2}

Table S-8: Data for the reaction of PQ and MeReO(mtp)L, where L = 4-phenylpyridine

[MeReO(mtp)L]/M	[L]/M	[PQ]/M	k_e/s^{-1}	Abs_{M-Cat}/cm^{-1}
3.0×10^{-3}	1.5×10^{-1}	3.0×10^{-5}	9.53×10^{-4}	1.31×10^{-1}
3.0×10^{-3}	1.2×10^{-2}	3.0×10^{-5}	3.43×10^{-4}	4.01×10^{-1}
3.0×10^{-3}	1.5×10^{-2}	3.0×10^{-5}	3.51×10^{-4}	3.99×10^{-1}
3.0×10^{-3}	9.0×10^{-2}	3.0×10^{-5}	6.53×10^{-4}	1.84×10^{-1}
3.0×10^{-3}	6.0×10^{-2}	3.0×10^{-5}	5.26×10^{-4}	2.34×10^{-1}
3.0×10^{-3}	2.0×10^{-2}	3.0×10^{-5}	3.77×10^{-4}	3.63×10^{-1}
3.0×10^{-3}	3.0×10^{-2}	3.0×10^{-5}	4.25×10^{-4}	3.20×10^{-1}
3.0×10^{-3}	1.2×10^{-1}	3.0×10^{-5}	7.99×10^{-4}	1.50×10^{-1}
1.0×10^{-3}	6.0×10^{-2}	3.0×10^{-5}	3.59×10^{-4}	1.17×10^{-1}
2.0×10^{-3}	1.4×10^{-1}	3.0×10^{-5}	7.95×10^{-4}	1.00×10^{-1}
2.0×10^{-3}	1.6×10^{-1}	3.0×10^{-5}	8.95×10^{-4}	8.83×10^{-2}

Table S-9: Data for the reaction of PQ and MeReO(mtp)L, where L = 4-picoline

[MeReO(mtp)L]/M	[L]/M	[PQ]/M	k_e/s^{-1}	Abs_{M-Cat}/cm^{-1}
3.0×10^{-3}	1.2×10^{-2}	3.0×10^{-5}	2.85×10^{-4}	3.61×10^{-1}
6.0×10^{-3}	2.4×10^{-2}	3.0×10^{-5}	5.37×10^{-4}	3.57×10^{-1}
9.0×10^{-3}	3.6×10^{-2}	3.0×10^{-5}	7.68×10^{-4}	3.45×10^{-1}
3.0×10^{-3}	9.7×10^{-2}	3.0×10^{-5}	7.01×10^{-4}	1.29×10^{-1}
3.0×10^{-3}	1.5×10^{-1}	3.0×10^{-5}	1.04×10^{-3}	8.79×10^{-2}
3.0×10^{-3}	3.0×10^{-2}	3.0×10^{-5}	3.42×10^{-4}	2.66×10^{-1}
3.0×10^{-3}	6.0×10^{-2}	3.0×10^{-5}	5.37×10^{-4}	1.68×10^{-1}
3.0×10^{-3}	1.2×10^{-1}	3.0×10^{-5}	8.07×10^{-4}	1.10×10^{-1}
3.0×10^{-3}	4.0×10^{-2}	3.0×10^{-5}	3.85×10^{-4}	2.31×10^{-1}
3.0×10^{-3}	2.0×10^{-2}	3.0×10^{-5}	2.81×10^{-4}	3.19×10^{-1}
3.0×10^{-3}	1.5×10^{-2}	3.0×10^{-5}	2.61×10^{-4}	3.51×10^{-1}

Table S-10: Data for the reaction of PQ and MeReO(mtp)L, where L = pyridine

[MeReO(mtp)L]/M	[L]/M	[PQ]/M	k_e/s^{-1}	Abs_{M-Cat}/cm^{-1}
9.0×10^{-3}	8.1×10^{-2}	3.0×10^{-5}	1.68×10^{-3}	7.37×10^{-2}
6.0×10^{-3}	7.2×10^{-2}	3.0×10^{-5}	1.20×10^{-3}	1.91×10^{-1}
6.0×10^{-3}	9.0×10^{-2}	3.0×10^{-5}	1.27×10^{-3}	1.80×10^{-1}
3.0×10^{-3}	6.0×10^{-2}	3.0×10^{-5}	6.57×10^{-4}	3.10×10^{-1}
3.0×10^{-3}	1.2×10^{-1}	3.0×10^{-5}	8.83×10^{-4}	2.45×10^{-1}
3.0×10^{-3}	1.5×10^{-1}	3.0×10^{-5}	1.01×10^{-3}	2.19×10^{-1}
3.0×10^{-3}	1.8×10^{-1}	3.0×10^{-5}	1.12×10^{-3}	1.95×10^{-1}
3.0×10^{-3}	3.0×10^{-1}	3.0×10^{-5}	1.56×10^{-3}	1.31×10^{-1}

Table S-11: Data for the reaction of DBQ and MeReO(mtp)L, where L = pyridine

[MeReO(mtp)L]/M	[L]/M	[DBQ]/M	k_e/s^{-1}	Abs_{M-Cat}/cm^{-1}
2.0×10^{-3}	1.8×10^{-2}	6.0×10^{-5}	1.60×10^{-2}	1.056
2.0×10^{-3}	2.4×10^{-2}	6.0×10^{-5}	1.64×10^{-2}	1.044
1.0×10^{-3}	1.5×10^{-2}	6.0×10^{-5}	7.25×10^{-3}	1.028
1.0×10^{-3}	2.0×10^{-2}	6.0×10^{-5}	7.58×10^{-3}	1.039
1.0×10^{-3}	4.0×10^{-2}	6.0×10^{-5}	9.33×10^{-3}	1.036
6.0×10^{-4}	3.0×10^{-2}	6.0×10^{-5}	4.87×10^{-3}	1.032
6.0×10^{-4}	3.6×10^{-2}	6.0×10^{-5}	5.93×10^{-3}	1.035
6.0×10^{-4}	6.0×10^{-2}	6.0×10^{-5}	4.36×10^{-3}	1.030
3.0×10^{-3}	2.7×10^{-2}	6.0×10^{-5}	2.59×10^{-2}	1.002
2.5×10^{-3}	2.25×10^{-2}	6.0×10^{-5}	2.16×10^{-2}	0.987
1.5×10^{-3}	1.35×10^{-2}	6.0×10^{-5}	1.25×10^{-2}	0.990
8.0×10^{-4}	7.2×10^{-3}	6.0×10^{-5}	5.95×10^{-3}	0.965

Table S-12: Data for the reaction of DBQ and MeReO(mtp)L, where L = 4-*tert*-butylpyridine

[MeReO(mtp)L]/M	[L]/M	[DBQ]/M	k_e/s^{-1}
6.0×10^{-4}	5.4×10^{-3}	6.0×10^{-5}	2.87×10^{-3}
8.0×10^{-4}	7.2×10^{-3}	6.0×10^{-5}	2.97×10^{-3}
1.0×10^{-3}	9.0×10^{-3}	6.0×10^{-5}	3.98×10^{-3}
1.5×10^{-3}	1.35×10^{-2}	6.0×10^{-5}	5.84×10^{-3}
2.0×10^{-3}	1.8×10^{-2}	6.0×10^{-5}	8.01×10^{-3}
2.5×10^{-3}	2.25×10^{-2}	6.0×10^{-5}	1.01×10^{-2}
3.0×10^{-3}	2.7×10^{-2}	6.0×10^{-5}	1.22×10^{-2}

The values of Abs_{M-Cat}/cm^{-1} were not available with this ligand because the decomposition of MeReO(mtp)DBCat was too fast.

References

1)Jacob, J.; Guzei, I. A.; Espenson, J. H. *Inorg. Chem.* 1999, *38*, 1040-1041.

2)Jacob, J.; Guzei, I. A.; Espenson, J. H. *Inorg. Chem.* 1999, *38*, 3266-3267.

3)Shan, X.; Espenson, J. H. , unpublished information.

4)Huang, R.; Espenson, J. H. *Chem. Commun.* 2000, submitted for publication.

5)Wang, Y.; Espenson, J. H. *Org. Lett.* 2000, *2*, 3525-3526.

6)Jacob, J.; Lente, G.; Guzei, I. A.; Espenson, J. H. *Inorg. Chem.* 1999, *38*, 3762-3763.

7)Lente, G.; Guzei, I. A. *Inorg. Chem.* 2000, *39*, 1311-1319.

8)Lippard, S. J.; Berg, J. M. *Principles of Bioinorganic Chemistry*; University Science Books: Mill Valley, CA, 1994, pp 71-72.

9)Campbell, N. A. *Biology*; 2nd ed.; The Benjamin/Cummings Publishing Company, Inc.: Redwood City, CA, 1990, p 925, 993.

10)Abrams, M. J.; Juweid, M.; ten Kate, C. I.; Schwartz, D. A.; Hauser, M. M.; Gaul, F. E.; Fuccello, A. J.; Rubin, R. H.; Strauss, H. W.; Fischman, A. J. *J. Nucl. Med.* 1990, *31*, 2022-2028.

11)Abrams, M. J.; Shaikh, S. N.; Zubeita, J. *Inorg. Chim. Acta* 1990, *173*, 133-135.

12)Abrams, M. J.; Larsen, S. K.; Zubieta, J. *Inorg. Chim. Acta* 1990, *171*, 133-134.

13)Abrams, M. J.; Chen, Q.; Shaikh, S. N.; Zubieta, J. *Inorg. Chim. Acta* 1990, *176*, 11-13.

14)Abrams, M. J.; Larsen, S. K.; Shaikh, S. N.; Zubieta, J. *Inorg. Chim. Acta* 1991, *185*, 7-15.

15)Davison, A.; DePamphilis, B. V.; Jones, A. G.; Franklin, K. J.; Lock, C. J. L. *Inorg. Chim. Acta* 1987, *128*, 161-167.

16)Kettler, P. B.; Chang, Y.-D.; Zubieta, J.; Abrams, M. J. *Inorganica Chimica Acta* **1994**, *218*, 157-65.

17)Edwards, C. F.; Griffith, W. P.; White, A. J. P.; Williams, D. J. *J. Chem. Soc., Dalton Trans.* **1992**, 957-962.

18)Herrmann, W. A.; Kusthardt, U.; Herdtweck, E. *J. Organomet. Chem.* **1985**, *294*, C33-C36.

19)Dilworth, J. R.; Griffiths, D. V.; Parrott, S. J.; Zheng, Y. *J. Chem. Soc., Dalton Trans.* **1997**, 2931-2936.

20)deLearie, L. A.; Pierpont, C. G. *J. Am. Chem. Soc.* **1986**, *108*, 6393-6394.

21)deLearie, L. A.; Haltiwanger, R. C.; Pierpont, C. G. *Inorg. Chem.* **1987**, *26*, 817-821.

22)Dilworth, J. R.; Ibrahim, S. K.; Khan, S. R.; Hursthouse, M. B.; Karaulov, A. A. *Polyhedron* **1990**, *9*, 1323-1329.

23)Creber, K. A. M.; Wan, J. K. S. *J. Am. Chem. Soc.* **1981**, *103*, 2101-2102.

24)Takacs, J.; Cook, M. R.; Kiprof, P.; Kuchler, J. G.; Herrmann, W. A. *Organometallics* **1991**, *10*, 316-320.

25)Lam, W. W. Y., Unpublished Results.

26)Lente, G.; Shan, X.; Guzei, I. A.; Espenson, J. H. *Inorg. Chem.* **2000**, *39*, 3572-3576.

27)Zékány, L.; Nagypál, I. "*PSEQUAD A Comprehensive Program for the Evaluation of Potentiometric and/or Spectrophotometric Equilibrium Data Using Analytical Derivatives*" in *Computational Methods for the Determination*

of Formation Constants; Legett, D. J., Ed.; Plenum Press: New York, 1985, pp 291-353. We are grateful to Gábor Lente for assistance in its implementation.

28)*Scientist;* version 2.0 ed.; Micromath Software, 1995.

29)Rockey, T. M.; Espenson, J. H. , Unpublished information.

30)Ugi, I.; Marquarding, D.; Klusacek, H.; Gillespie, P. *Acc. Chem. Res.* 1971, 4, 288-296.

31)Casares, J. A.; Espinet, P. *Inorg. Chem.* 1997, 36, 5428-5431.

32)Lee, J. C.; Yao, W.; Crabtree, R. H. *Inorg. Chem.* 1996, 35, 695-699.

33)Espinet, P.; Hernando, R.; Iturbe, G.; Villafane, F.; Orpen, A. G.; Pascual, I. *Eur. J. Inorg. Chem.* 2000, 1031-1038.

34)Gallop, M. A.; Johnson, B. F. G.; Keeler, J.; Lewis, J.; Heyes, S. J.; Dobson, C. M. *J. Am. Chem. Soc.* 1992, 114, 2510-2520.

35)Lahti, D. W.; Espenson, J. H. *Submitted for publication* .

36)Lente, G.; Jacob, J.; Guzei, I. A.; Espenson, J. H. *Inorg. React. Mech.* 2000, in press.

37)Pierpont, C. G.; Lange, C. W. *Progress in Inorganic Chemistry* 1994, 41, 331-442.

38)Abu-Omar, M. M.; Hansen, P. J.; Espenson, J. H. *J. Am. Chem. Soc.* 1996, 118, 4966-4974.

39)Espenson, J. H.; Pestovsky, O.; Huston, P.; Staudt, S. *J. Am. Chem. Soc.* 1994, 116, 2869-2877.

40)Yamazaki, S.; Espenson, J. H.; Huston, P. *Inorg. Chem.* 1993, 32, 4683-4687.

41)Herrmann, W. A.; Fischer, R. W.; Scherer, W.; Rauch, M. U. *Angew. Che., Int. Ed. Engl.* 1993, 32, 1157-1160.

42)Eager, M. D.; Espenson, J. H. *Inorg. Chem.* **1999**, *38*, 2533-2535.

CHAPTER 2

KINETICS AND MECHANISMS OF REACTIONS OF ALKYL

HYDROPEROXIDES WITH METHYLRHENIUM OXIDES

A paper published in Inorganic Chemistry*

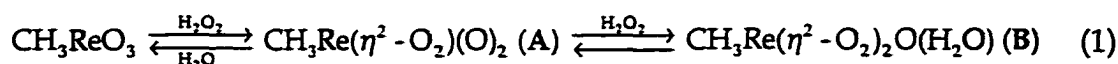Kimberly A. Brittingham and James H. Espenson

Abstract

Aqueous methyldioxorhenium (MDO), prepared from methyltrioxorhenium (MTO) and hypophosphorous acid, abstracts an oxygen atom from tertiary alkyl hydroperoxides This regenerates MTO and forms the tertiary alcohol with rate constants 3.71×10^4 L mol^{-1} s^{-1} (t-BuOOH) and 3.47×10^4 L mol^{-1} s^{-1} (t-AmOOH) at 25.0 °C in aqueous 1.0 M HOTf. MDO reacts with hydrogen peroxide first to form MTO, $k = 3.36 \times 10^4$ L mol^{-1} s^{-1}, which subsequently reacts with more hydrogen peroxide to form peroxorhenium complexes. In a separate study, the concomitant slow decomposition of alkyl hydroperoxides and MTO (to ReO_4^-) was investigated. The rate law is $v = k[MTO][RCMe_2OOH]/[H^+]$, with $k = 7.4 \times 10^{-5}$ s^{-1} (R = Me) and $k = 8.4 \times 10^{-5}$ s^{-1} (R = Et) at 25.0 °C in aq. solution at μ 1.0 M. ^{1}H NMR spectroscopy and GC revealed organic products suggestive of radical reactions. The products from t-BuOOH are acetone, methanol, tert-butyl methyl ether, methane, ethane, and tert-butyl methyl peroxide. With CH_2DReO_3, it could be shown that both t-BuOOH and MTO were sources of the methane. The rate of decomposition of MTO shows an inverse-first-order dependence on [H$^+$] throughout the range pH 1-6.42.

Introduction

An extensive amount of literature now describes how hydrogen peroxide and MTO (CH_3ReO_3) form two η^2-peroxorhenium species, $A = CH_3Re(\eta^2\text{-}O_2)(O)_2$ and $B = CH_3Re(\eta^2\text{-}O_2)_2(O)(H_2O)$, eq 1.[1-4] Both are active catalysts for hydrogen peroxide oxidations.[5]

$$CH_3ReO_3 \underset{H_2O}{\overset{H_2O_2}{\rightleftharpoons}} CH_3Re(\eta^2\text{-}O_2)(O)_2 \ (A) \overset{H_2O_2}{\underset{}{\rightleftharpoons}} CH_3Re(\eta^2\text{-}O_2)_2O(H_2O) \ (B) \qquad (1)$$

In solutions containing hydrogen peroxide, MTO is prone to irreversible decomposition by the nucleophilic hydroperoxide anion, HO^{2-} (eq 2)[6] and OH^- (eq 3)[6,7].

$$HO_2^- + CH_3ReO_3 \rightarrow CH_3OH + ReO_4^- \qquad (2)$$

$$OH^- + CH_3ReO_3 \rightarrow CH_4 + ReO_4^- \qquad (3)$$
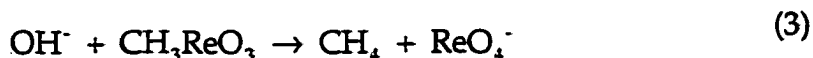
The rhenium(V) compound methyldioxorhenium (MDO, solvated or ligated) abstracts an oxygen atom from many oxygen donors XO:[7-9] $XO + CH_3ReO_2 \rightarrow X + CH_3ReO_3$, driven by the strength of the rhenium-oxygen bond in MTO, 464 kJ mol^{-1}.[9] Hydrogen peroxide converts MDO into the peroxo complexes A and B. Alkyl hydroperoxides, on the other hand, yield only MTO, allowing a kinetic analysis of the first stage:

$$ROOH + CH_3ReO_2 \rightarrow ROH + CH_3ReO_3 \ (k_4) \qquad (4)$$
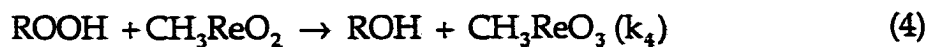
The slow decomposition of CH_3ReO_3 in aqueous solutions containing Me_3COOH (t-BuOOH) or $EtCMe_2OOH$ (t-AmOOH) has been studied. The different rhenium and organic products were used to assign a mechanism that clearly

involves free radicals. Cumyl hydroperoxide, $C_6H_5(CH_3)_2COOH$, is decomposed heterolytically by MTO in chlorobenzene; <1% of the process involves radicals.[10]

Experimental Section

Materials. A Millipore-Q water purification system provided high purity water. Deuterium oxide (99%) was used as the NMR solvent. Solutions were acidified with trifluoromethanesulfonic acid (HOTf, triflic acid) diluted from the commercially available material (98%). Perchloric acid or its salts could not be present, owing to the reaction between MDO and ClO_4^-.[8] Where needed, ionic strength was maintained with lithium triflate.

t-Butyl hydroperoxide was obtained commercially as a 70% solution in water. *t*-Amyl hydroperoxide was synthesized and analyzed as previously described.[11] CH_2DReO_3 was synthesized from dirhenium heptoxide, trifluoroacetic acid, and $CH_2DSn(n\text{-butyl})_3,$[12] which was kindly donated by Dr. Michael T. Ashby. Other reagents were available commercially: MTO, hypophosphorous acid (50% in water), phosphorous acid, *t*-butyl alcohol, hydrogen peroxide (30% in water), *t*-amyl alcohol, 2-methyl-1-phenyl-2-propanol, HPLC grade acetonitrile, dirhenium heptoxide, and trifluoroacetic acid. Methyldioxorhenium (MDO) was generated in situ from hypophosphorous acid and MTO in strongly acidic aqueous solution,

$k_5 = 2.8 \times 10^{-2}$ L mol^{-1} s^{-1} at 25.0 °C:[9]

$$CH_3ReO_3 + H_3PO_2 \rightarrow CH_3ReO_2 + H_3PO_3 \ (k_5) \tag{5}$$

With higher (~10 mM) concentrations of MDO for NMR studies, a blue color indicated the onset of MDO oligomerization.[8,9] The addition of alkyl hydroperoxide immediately restored colorless MTO. We surmise that the disappearance of oligomer in this case is analogous to the reduction of perchlorate ions by dimeric

$MDO.^{[8]}$ Oligomerization might have been largely avoided by maintaining pH 0, but this was not feasible because of NMR shimming difficulties.

Instrumentation. Spectrophotometric data were recorded using Shimadzu UV-2501PC and UV-3101PC spectrophotometers. Kinetic data for fast reactions were collected with an Applied Photophysics Sequential DS-17MV stopped-flow spectrophotometer. ^{1}H NMR spectroscopy was used to monitor MTO (s, 2.46 ppm) and the increase in organic products over time in D_2O. The ^{1}H NMR spectra were obtained with Varian VXR-300 or Bruker DRX-400 spectrometers, using acetonitrile as an internal standard (d, 2.09 ppm). ^{31}P spectra were referenced to 85% H_3PO_4. ^{1}H NMR kinetics were recorded with the Bruker spectrometer at 22.5 ± 0.2 °C. The chemical shifts of the proton resonances for the organic reactants and products are as follows:

$(CH_3)_2CO$ δ 2.25 (s, 6H)

$(CH_3)_3COH$ δ 1.271 (s,9H)

$(CH_3)_3COCH_3$ δ 3.25 (s, 3H)

CH_3OOH δ 3.887 (s, 3H)

$(CH_3)_3COOH$ δ 1.266 (s, 9H)

CH_3OH δ 3.37 (s, 3H)

$(CH_3)_3COOCH_3$ δ 3.86 (s, 3H)

CH_2O δ 5.092 (s, 2H)

$CH_3CH_2(CH_3)_2COOH$ δ 0.893 (t, 3H)

$CH_3CH_2(CH_3)_2COOH$ δ 1.601 (q, 2H)

$CH_3CH_2(CH_3)_2COOH$ δ 1.215 (s, 6H)

$CH_3CH_2(CH_3)_2COH$ δ 0.86(t, 3H)

$CH_3CH_2(CH_3)_2COH$ δ 1.485 (q, 2H)

$CH_3CH_2(CH_3)_2COH$ δ 1.166 (s, 6H)

$CH_3CH_2(CH_3)_2COCH_3$ δ 3.217 (s, 3H)

$CH_3CH_2(CH_3)_2COOCH_2CH_3$ δ 3.678 (q, 2H)

The chemical shifts for the commercially available compounds were assigned on the basis of authentic sample. The CH_3OOH was prepared by literature methods.[13] The $(CH_3)_3COOCH_3$ was prepared from dimethyl sulfate and *tert*-butylhydroperoxide on the basis of the same procedure.[13] A quartet resonance among the products of the reaction of t-AmOOH and MTO is the result of an unassigned methylene group of an ethyl group that has been shifted downfield by an oxygen. We take this

resonance to be that of *tert*-amyl ethyl peroxide because the *t*-BuOOH reaction forms the analogous dialkyl peroxide.

Methane, ethane, ethylene and propane were determined by gas chromatography on a VZ-10 column. Perrhenate ions were detected with a Perkin-Elmer Sciex API electrospray mass spectrometer with a syringe injector. GC-MS experiments were performed with a TSQ700 mass spectrometer (Finnigan MAT). The mass spectra were obtained by scanning the first quadrupole from m/z 10 to m/z 20 for 0.5 second. The 2nd and 3rd quadrupoles were maintained in the RF only mode. The system was configured in the electron impact ionization mode. A DB1 column was used. The injector and transfer-line temperatures were maintained at 260 °C and 240 °C, respectively.

Results

Kinetics of the reaction of MDO with ROOH. Kinetic data were obtained with the stopped-flow technique at 25.0 ± 0.2 °C in aqueous solution. The MDO solution was prepared from MTO and hypophosphorus acid in one of the SF syringes containing HOTf and/or LiOTf. After 5 half-lives for MDO formation had elapsed, $k_5 = (2.8 \pm 0.2) \times 10^{-2}$ L mol^{-1} s^{-1}, the MDO solution was mixed in the SF apparatus with the contents of the other syringe holding the appropriate concentrations of ROOH, HOTf and LiOTf. The buildup of MTO was monitored at 270 nm ($\varepsilon = 1300$ L mol^{-1} cm^{-1}). The reactant concentrations were varied over these ranges: 50-200 µM MDO and 0.5-10 mM *tert*-BuOOH. In addition, the concentrations of H_3PO_2 and H^+ were varied modestly: 0.05-0.1 M and 0.032-1.0 M, respectively, to confirm the absence of kinetic effects from these variables. Ionic strength was maintained at 1.0 M with lithium triflate. The absorbance-time data in

each experiment were fit to first-order kinetics, eq 6, since the alkyl hydroperoxide was taken in substantial excess.

$$Abs_t = Abs_\infty + (Abs_0 - Abs_\infty)e^{-k_\psi t} \tag{6}$$

The variation of k_ψ with $[t\text{-BuOOH}]_{av}$ is presented in Figure 1. A linear least-squares fit gave k_4 at 25.0 °C as the slope: $(3.71 \pm 0.10) \times 10^4$ L mol^{-1} s^{-1}. For t-AmOOH, $k_4 = (3.47 \pm 0.07) \times 10^4$ L mol^{-1} s^{-1}.

The reactions in eqs 4 and 5 constitute a catalytic cycle, the faster step destroying the MDO and the other reforming it more slowly. In effect, then, MTO catalyzes the reaction between hypophosphorous acid and alkyl hydroperoxide:

$$ROOH + H_3PO_2 \xrightarrow{\text{cat. MTO}} ROH + H_3PO_3 \tag{7}$$

This is a spontaneous reaction in the thermodynamic sense, but it does not occur under these conditions without a catalyst. In the course of checking the catalytic reaction, other reactions were found to take place concurrently over longer times (here limited by the lower rate of reaction 5). The additional reactions entailed the concurrent decomposition of MTO and ROOH, as discussed later.

Kinetics of the reaction of MDO with H_2O_2. In principle, these experiments were the same as those just reported for ROOH, except that reaction 4 is followed by others, leading to further products, eq 1. When MDO ($[MTO]_0 = 0.1$ mM, $[H_3PO_2]_0 = 50$ mM) was mixed with H_2O_2 (10 mM), the absorbance at 270 nm for MTO increased with time according to first-order kinetics. For that stage, the rate constant for the reaction between MDO and H_2O_2 is $k_4 = (3.36 \pm 0.02) \times 10^4$ L mol^{-1} s^{-1}. Over longer times, the formation of B was monitored at 360 nm. The pseudo-first-order rate constant of this second component agreed with that determined directly for
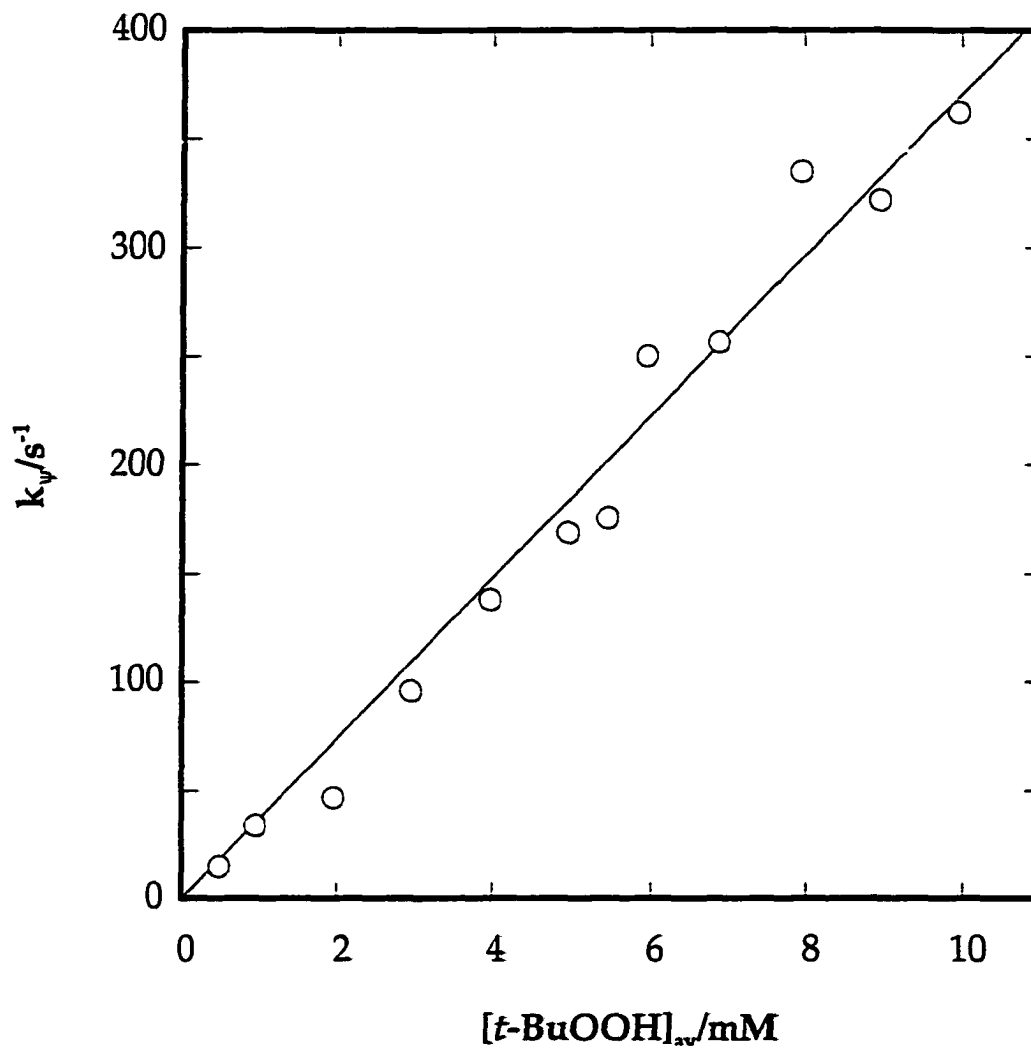
Figure 1. Kinetic data for the reaction of *tert*-butyl hydroperoxide with methyldioxorhenium in aqueous solutions of triflic acid (0-1.0 M) at 25.0 °C and ionic strength 1.0 M. Shown is a plot of the pseudo-first-order rate constant against the average concentration of the hydroperoxide, the reagent in excess.

H_2O_2 + MTO. These findings provide spectroscopic and kinetic evidence that MTO was formed in the first step.

Kinetics of the concurrent decomposition of MTO and $RCMe_2OOH$. In the strongly acidic medium needed to stabilize MDO, pH 0-1, MTO remains fairly stable without the hydroperoxide. With the hydroperoxide, however, both MTO and the alkyl hydroperoxide slowly decompose *concurrently* at a pH-dependent rate.

The decomposition of MTO (0.5 mM) by $RCMe_2OOH$ (10 mM) was monitored spectrophotometrically at 270 nm over at pH 1.0-6.42. The data were fit to first-order kinetics at each pH. Values of an apparent second-order rate constant were calculated as $k_{app} = k_\psi/[RCMe_2OOH]$. The plot of log k_{app} versus pH was linear, Figure 2 inset, with a slope of 0.93 ± 0.03. Thus the decomposition is inverse-first-order with respect to [H$^+$]. Reactions of t-AmOOH were monitored at pH 1, 2, and 3.25. The pattern closely resembles that of t-BuOOH. The rate equation for both is

$$v = k_f \frac{[MTO][RCMe_2OOH]}{[H^+]} \tag{8}$$

The plot of k_{app} versus 1/[H$^+$] is linear, Figure 2. The data in this plot were taken from experiments at ionic strengths of 0.05 M and 1.0 M. The k_f values from these fits are (7.4 ± 0.1) × 10^{-5} s^{-1} (t-BuOOH) and (8.4 ± 0.4) × 10^{-5} s^{-1} (t-AmOOH) at 25.0 °C.

^{1}H NMR was used to study the dependence of the same reaction (μ = 0.1 M, [H$^+$] = 0.1 M) on [t-BuOOH] at 22.5 °C. The values of k_ψ for the disappearance of MTO were plotted against [t-BuOOH] to give k_{app} = (2.41 ± 0.07) × 10^{-4} L mol^{-1} s^{-1}, where $k_{app} = k_f/[H^+]$. Therefore, according to these NMR experiments, k_f = (2.41 ± 0.07) × 10^{-5} s^{-1}. These values for k_f, as determined by UV-Vis spectrophotometry and
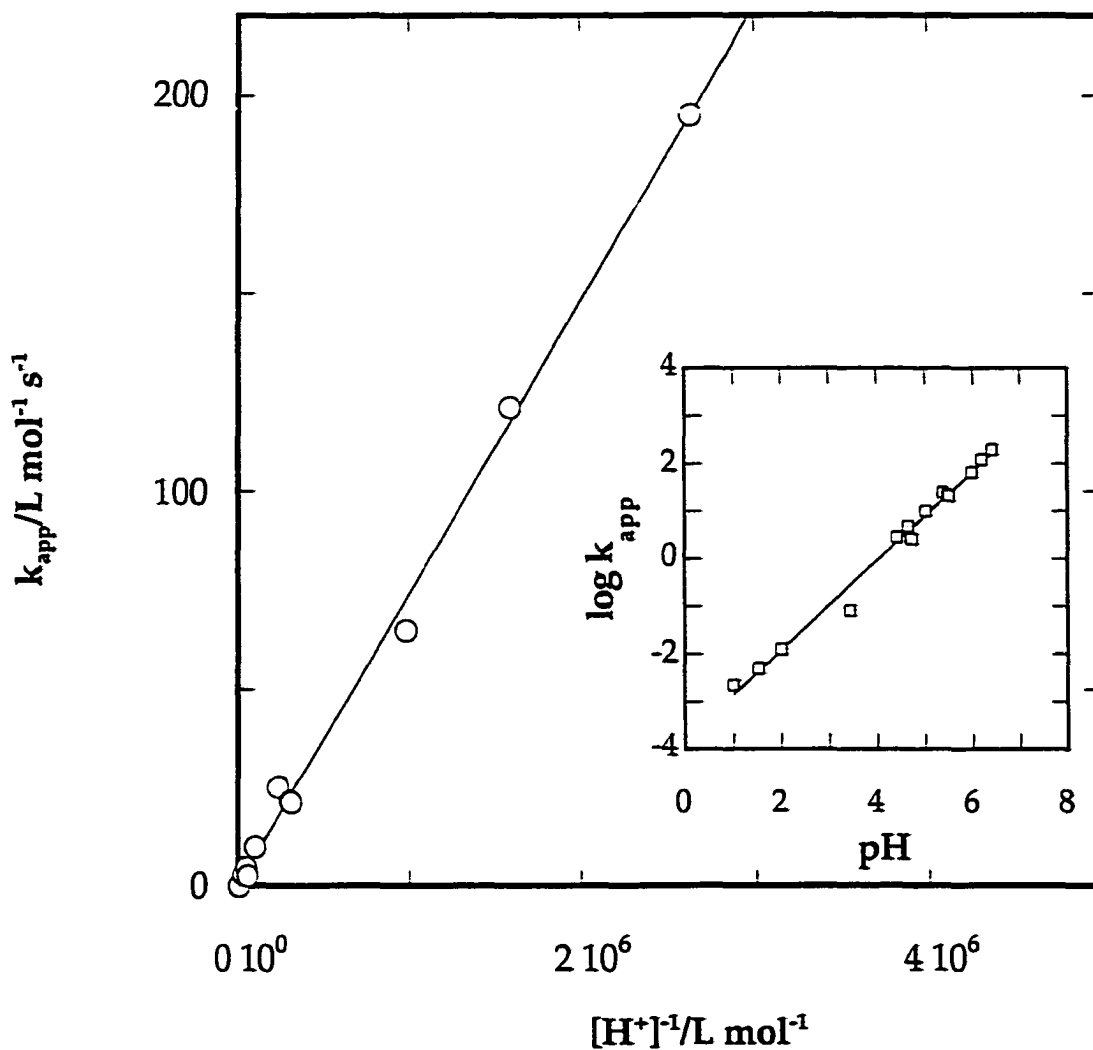
Figure 2. Dependence of second order-rate constant, k_{app}, on $1/[H^+]$ at 25 °C. Slope is $k_t = (7.4 \pm 0.1) \times 10^{-5}$ s^{-1}. Inset shows a plot of log k_{app} vs pH, with a slope 0.93 $\pm$ 0.03. The points at pH 1, 2, 3.44, and 4.72 were at $\mu = 1.0$ M; the others were at $\mu = 0.05$ M.

NMR, differ by a factor of three. This discrepancy arises from the use of quite different ranges of reactant concentrations, a different experimental technique, a different reaction medium, and a modestly different temperature.

Products of decomposition of MTO and *t*-BuOOH. The decomposition of MTO and *t*-BuOOH might be anticipated to parallel reaction 2. Perrhenate ions and *tert*-butyl methyl ether would be the products from attack of the *tert*-butyl peroxide anion on MTO. These products were indeed found, but others were formed as well. The loss of MTO and *t*-BuOOH under an Ar atmosphere was monitored by NMR. GC was also employed to detect the alkanes in the gas phase. The products included $(CH_3)_2CO$, CH_3OH, *tert*-$BuOCH_3$, CH_4, C_2H_6 and *tert*-$BuOOCH_3$. Although *tert*-BuOH is seen as a product by ^1H NMR, its signal overlaps that for *tert*-BuOOH, and therefore the change in its peak intensity could not be monitored. The perrhenate ion has also been qualitatively detected using electrospray mass spectroscopy. The initial concentrations were: ~10 mM MTO, 200 mM *t*-BuOOH, 100 mM HOTf and 10 mM CH_3CN as the NMR standard. The reagents were added except *t*-BuOOH, and the NMR spectrum recorded. Then *t*-BuOOH was added and the spectrum recorded over approximately 4 h. The concentration-time data for the decrease in MTO and the increase in reaction products were fit to first-order kinetics. The rate constants are reported in Table 1.

According to Table 1, the pseudo-first-order rate constants for the decomposition of MTO and the build up of methanol, acetone, *tert*-butyl methyl ether, and *tert*-butyl methyl peroxide are the same within error. The weighted mean[14] of these first-order rate constants is $k_{dec} = (5.76 \pm 0.05) \times 10^{-5} \text{ s}^{-1}$. Table 1 also reports the final concentration of each product. It is difficult to calculate the mass

Table 1. Rate Constants for the Decrease of MTO and Increase of Products During the Decomposition of MTO (17 mM) and t-BuOOH (200 mM) at 22.5 ± 0.2 °C.

Species	$k_{dec}/10^{-5}$ s^{-1}	Final Conc.[a]/mM
MTO	6.2 ± 0.2	0.4 ± 0.1
CH_3OH	5.55 ± 0.07	4.44 ± 0.02 (26%) [b]
$(CH_3)_2CO$	6.1 ± 0.1	2.78 ± 0.2 (16%)
t-BuOCH$_3$	5.9 ± 0.1	2.37 ± 0.02 (14%)
t-BuOOCH$_3$	5.2 ± 0.2	1.85 ± 0.04 (11%)

[a] From least squares fitting of the experimental data; [b] Percent yield relative to $[MTO]_0$.

balance of products because of the complicated radical decomposition process, which is discussed later.

Methane and ethane were monitored by gas chromatography. MTO (10 mM) and t-BuOOH (200 mM) were mixed together in 0.1 M HOTf at room temperature. The total volume of solution was 7 mL. The reaction was carried out in a 20 mL bottle sealed with a septum. No care was taken to exclude oxygen. The solution was shaken vigorously, and then the head space was injected into the GC. Data seemed to indicate that the rates of buildup of these products was several times faster than those detected by NMR spectroscopy. It should be noted that these experiments were done to detect methane and ethane and are of qualitative significance only.

To determine whether MTO, or t-BuOOH, or both were a source of Me$^\bullet$, 98% CH_2DReO_3 was employed. The GC of the argon saturated-solution indicated peaks for methane and water. The MS of the methane peak showed a significant amount of the CH_3D^+ ion at m/z 17. It was not possible to determine the ratio CH_3D/CH_4 to sufficient accuracy, but it was evident that both were present. Thus, the methane is composed of methyl radical that is partly derived from the β-scission of the *tert*-butoxyl radical and partly from MTO decomposition.

Products of the decomposition of MTO and t-AmOOH. Acetone, methanol, methane, ethane, *tert*-amyl methyl ether, and *tert*-amyl ethyl peroxide were found, along with small amounts of ethylene and propane. The rate constants for the products detected by NMR, Table 2, show a weighted mean [14] of $(2.36 \pm 0.04) \times 10^{-4}$ s^{-1}.

Table 2. Rate Constants for the Decrease of MTO and Increase of Products During the Decomposition of MTO (7.0 mM) and t-AmOOH (200 mM) at 22.5 ± 0.2 °C.

Species	$k_{dec}/10^{-4} \, s^{-1}$	Final Conc.[a]/mM
MTO	2.13 ± 0.08	1.2 ± 0.1
CH_3OH	2.53 ± 0.07	3.89 ± 0.05 (56%)[b]
$(CH_3)_2CO$	1.7 ± 0.2	5.21 ± 0.05 (74%)
t-AmOCH$_3$	2.59 ± 0.07	0.83 ± 0.02 (12%)
t-AmOOCH$_2$CH$_3$	1.3 ± 0.2	4.0 ± 0.7 (57%)

[a] From least squares fitting of the experimental data; [b] Percent yield relative to $[MTO]_0$.

The GC analysis was carried out the same as for t-BuOOH. The values of k_{dec} from the first-order fits are: $(5.7 \pm 0.4) \times 10^{-4} \, s^{-1}$ (CH_4), $(6.0 \pm 0.3) \times 10^{-4} \, s^{-1}$ (C_2H_6), $(6.0 \pm 0.6) \times 10^{-4} \, s^{-1}$ (C_2H_4), $(3.7 \pm 0.3) \times 10^{-4} \, s^{-1}$ (C_3H_8). These values are slightly higher than the weighted mean of the k_{dec} for the water soluble products, but are of the same order of magnitude.

Experiments in the Presence of Oxygen. The reaction between MTO (10 mM) and t-BuOOH (200 mM) under O_2 gave two additional organic products, methyl hydroperoxide and formaldehyde.
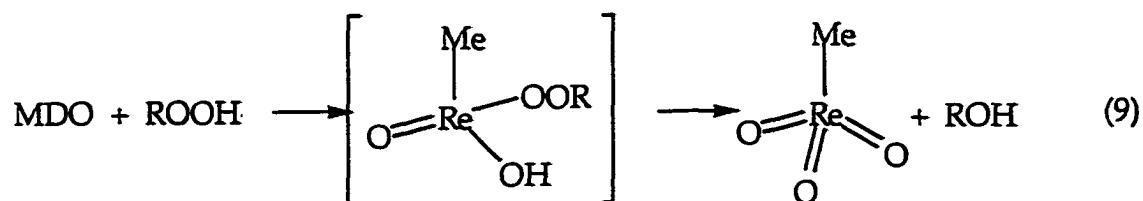
Phosphoric acid. No conditions have been found under which H_3PO_2 or H_3PO_3 could be oxidized to phosphate by MTO catalyzed reactions of hydrogen peroxide. To our surprise then, phosphoric acid was produced when t-BuOOH was added to a solution of MDO containing excess H_3PO_2. This experiment consisted of adding 200 mM t-BuOOH to a solution prepared from 10 mM MTO and 100 mM H_3PO_2 that had been allowed to stand for 88 seconds, in which time the blue color for MDO oligomerization became apparent. The ^{31}P NMR spectrum of this reaction mixture was used to substantiate H_3PO_3 (d, 5.49 ppm) and H_3PO_4 (s, 0.63 ppm).

Under these conditions, hypophosphorous acid and *tert*-butyl hydroperoxide do not react without MTO. Phosphoric acid was formed at approximately the same rate when H_3PO_2 was replaced by H_3PO_3. When chlorate ion, ClO_3^-, was used in place of t-BuOOH, phosphorous acid was the only product. These findings suggest that the precursor to phosphoric acid is phosphorous acid. Also, phosphoric acid formation is probably due to radical processes occurring in the t-BuOOH system because the effect was absent with ClO_3^-.

The rate constants for MTO loss and product buildup are given in Table 3. The weighted mean[14] of the rate constants for the loss of MTO and the buildup of methanol and *tert*-butyl methyl ether is $(12.9 \pm 0.3) \times 10^{-5}$ s^{-1}, which is about double that without H_3PO_2. Higher values of k_{dec} were found for acetone and *tert*-butyl methyl peroxide; the weighted mean is $(53.2 \pm 0.8) \times 10^{-5}$ s^{-1}. One exceptional finding is the following: the rate of acetone production, normalized by [MTO], is 14 times higher with H_3PO_2, and its final concentration 45 times greater.

Discussion

O-atom transfer. Reaction 4 represents O-atom transfer from the alkyl hydroperoxide to the MDO. For the transfer to occur, the alkyl hydroperoxide coordinates to MDO, to form a transient intermediate. This species is analogous to those first formed when MTO combines with various E-OH species (H-OH, H-OOH, R-OH, etc.).[6,7,12,15]

$$\text{MDO} + \text{ROOH} \longrightarrow \left[\begin{array}{c} \text{Me} \\ \text{O}{=}\text{Re}{\overset{\text{--OOR}}{\underset{\text{OH}}{\Big\langle}}} \end{array} \right] \longrightarrow \text{O}{=}\overset{\text{Me}}{\underset{\overset{\parallel}{\text{O}}}{\text{Re}}}{\big\langle}\text{O} + \text{ROH} \qquad (9)$$

Equations 4 and 9 account for rapid MTO buildup. One cannot say directly from the data whether the rate-controlling step is the coordination of the alkyl hydroperoxide or the breaking of the O-O bond. Given the high rate of MTO ligation reactions,[16] the rate-controlling step in reaction 9 seems most probably to be the breaking of the peroxide bond, as in the second step. The value of k_4 for *t*-BuOOH is only 7% larger than that for *t*-AmOOH, and the k_4 for H_2O_2 is slightly lower than that for either alkyl hydroperoxide. Two factors might contribute to

Table 3. Rate Constants and Final Concentrations for the Decomposition of MTO and the Buildup of Products in the Reaction of MTO (10 mM), H_3PO_2 (100 mM) and t-BuOOH (200 mM) at 22.5 ± 0.2 °C.[a]

Species	$k_{dec}/10^{-5} \, s^{-1}$	Final Conc.[b]/mM
MTO	15 ± 2	4.3 ± 0.2
CH_3OH	17.1 ± 0.8	$3.84 \pm 0.05 \, (38\%)$[c]
$(CH_3)_2CO$	50 ± 2	$73 \pm 2 \quad (730\%)$
t-BuOCH$_3$	9.4 ± 0.7	$0.88 \pm 0.02 \, (9\%)$
t-BuOOCH$_3$	54 ± 1	$2.46 \pm 0.03 \, (25\%)$

[a] $[HOTf]_0 = 100$ mM. [b] From least squares fitting of the experimental data; [c] Percent yield relative to $[MTO]_0$.

these small differences in k_4. The more electron-donating R group provides a more nucleophilic peroxide anion, and thus a larger k_4, if the first step is rate-controlling. Also, t-AmOOH is slightly more sterically hindered than t-BuOOH, but this is at best a minimal determinant of rate of MTO formation.
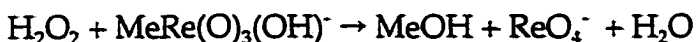
Kinetics of Decomposition of MTO and ROOH. The concurrent decomposition of MTO and H_2O_2 showed a $1/[H^+]$ kinetic dependence at $\mu = 0.05$ M. Methanol and perrhenate ions may be formed by one of these kinetically indistinguishable pathways:[6] (a) nucleophilic attack of HOO^- on MTO with $k_a = 2.03 \times 10^8$ L mol^{-1} s^{-1},

$$HOO^- + MeReO_3 \rightarrow [Me(O)_3Re\text{-}OOH]^- \rightarrow MeOH + ReO_4^-$$

(b) nucleophilic attack of OH^- on A with $k_b = 3.05 \times 10^9$ L mol^{-1} s^{-1},

$$OH^- + MeRe(O)_2(\eta^2\text{-}O_2) \rightarrow MeOH + ReO_4^-$$
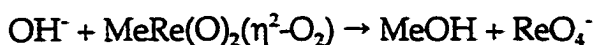
(c) a reaction between H_2O_2 and MTO-OH$^-$, the conjugate base of MTO ($pK_a = 7.5$)[15] with $k_c = 3.1 \times 10^5$ L mol^{-1} s^{-1},

$$H_2O_2 + MeRe(O)_3(OH)^- \rightarrow MeOH + ReO_4^- + H_2O$$

These considerations guide us to an interpretation of the kinetic data for ROOH. The rate constant for the decomposition of MTO by t-BuOOH is also proportional to $1/[H^+]$, as shown in Figure 2. This could be interpreted by mechanism (a) or (c), but not by (b) since that would require the same rate constant for H_2O_2 and $RCMe_2OOH$. The experimental pH dependence can be expressed by the rate law given by eq 10.
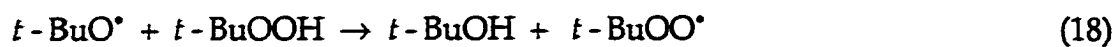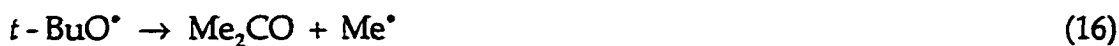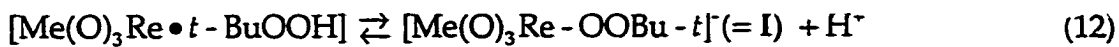
$$v = \frac{k_s K_a [MTO][ROOH]}{[H^+]} \tag{10}$$

If mechanism (a) prevails, then $pK_a = 12.8$ for t-BuOOH and $k_s = 4.6 \times 10^8$ L mol^{-1} s^{-1}.

If mechanism (c) provides the preferred pathway, then $pK_a = 7.5$ for MTO-OH$_2$[15]

and $k_s = 2.3 \times 10^3$ L mol^{-1} s^{-1}. In eq 10, k_s represents the corresponding bimolecular

rate constant for the mechanism indicated, k_a or k_c. k_s is related to k_f (eq 8) by the

relationship $k_f = k_s K_a$. Although credible arguments can be advanced for (a) over (c),

it is useful to consider an alternative that renders the distinction moot.[17] This

scheme involves a complex formed from MTO and ROOH in which the inductive

effect of rhenium (VII) enhances the acidity of the ROOH proton. This would lead

to the intermediate, I (R = t-Bu, t-Am). Its different cleavage reactions would lead to

the various products, as detailed in the next section.

$$
\begin{array}{c}
O \\
\| \\
O\!\!\diagdown\!\!\underset{Re}{\|}\!\!\diagup\!\!OOR \\
Me\diagup \quad \diagdown O^- \\
\end{array}
$$

I
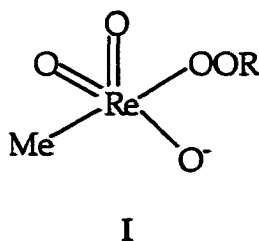
Decomposition of MTO and t-BuOOH. The proposed sequence of reactions

for the concomitant decomposition of MTO and t-BuOOH under argon is presented

in eqs 11-20 (Scheme 1). This is the simplest scheme we have been able to formulate

to account for the products and the pH dependence.

In this scheme, very rapid coordination of t-BuOOH to MTO to form a neutral

complex (eq 11) leads to the active intermediate I by acid ionization, eq 12. The

partitioning of I among three reactions leads to the products. Dissociation of I forms

t-BuOCH$_3$ and ReO$_4^-$, eq 13, cf. eq 2 with H$_2$O$_2$.[6] Formation of t-BuOCH$_3$ from

Scheme 1

$$MeReO_3 + t\text{-}BuOOH \rightarrow [Me(O)_3Re \bullet t\text{-}BuOOH] \tag{11}$$

$$[Me(O)_3Re \bullet t\text{-}BuOOH] \rightleftarrows [Me(O)_3Re\text{-}OOBu\text{-}t]^-(= I) + H^+ \tag{12}$$

$$I \rightarrow t\text{-}BuOMe + ReO_4^- \tag{13}$$

$$I + H_2O \rightarrow MeOH + t\text{-}BuOH + ReO_4^- \tag{14}$$

$$I \rightarrow t\text{-}BuO^\bullet + Me^\bullet + ReO_4^- \tag{15}$$

$$t\text{-}BuO^\bullet \rightarrow Me_2CO + Me^\bullet \tag{16}$$

$$Me^\bullet + t\text{-}BuOOH \rightarrow CH_4 + t\text{-}BuOO^\bullet \tag{17}$$

$$t\text{-}BuO^\bullet + t\text{-}BuOOH \rightarrow t\text{-}BuOH + t\text{-}BuOO^\bullet \tag{18}$$

$$2\,Me^\bullet \rightarrow C_2H_6 \tag{19}$$

$$Me^\bullet + t\text{-}BuOO^\bullet \rightarrow t\text{-}BuOOMe \tag{20}$$

t-BuO$^\bullet$ and CH$_3^\bullet$ must happen in the transition state or solvent cage, because separated t-BuO$^\bullet$ and CH$_3^\bullet$ remain at concentrations too low for bimolecular recombination. Cleavage of I to ReO$_4^-$, t-BuO$^\bullet$ and CH$_3^\bullet$, eq 15, accounts for t-BuO$^\bullet$, and also for the CH$_3^\bullet$ that is derived from the methyl group on MTO. Intermediate I undergoes peroxide bond homolysis; furthermore, the C-Re bond breaks to give the stable ReO$_4^-$. There is precedent for the bond homolysis of a metal hydroperoxide. The scheme proposed for the hydroxylation of cycloalkanes by ROOH using [Fe$^{III}_2$O(TPA)$_2$(H$_2$O)$_2$]$^{4+}$ involves O-O bond homolysis.[18] Reaction 15 was written as a single step for simplicity of the scheme, but it is more likely that it happens sequentially. Indeed, eqs 13 and 15 may not be independent reactions.[17] The third mode by which I reacts is hydrolysis to methanol, $tert$-butyl alcohol, and perrhenate ions, eq 14.

Other steps, all very fast, complete the sequence: the tert-butyoxyl radical and the methyl radical participate in a series of independently known steps, eqs 16-20, giving rise to acetone, methane, $tert$-butyl alcohol, ethane, and $tert$-butyl methyl peroxide. These products establish the involvement of methyl, alkoxyl and alkylperoxyl radicals. The BuO$^\bullet$ radical continues the free-radical chemistry by undergoing β-scission to form acetone and the methyl radical, eq 16, $k_{16} = 1.4 \times 10^6$ s^{-1}.[19] The methyl radical can then abstract H$^\bullet$ from the t-BuOOH to give methane and $tert$-butylperoxyl radical, eq 1.[20] The $tert$-butoxyl radical, itself, can also abstract a hydrogen atom from t-BuOOH to give $tert$-butyl alcohol and $tert$-butylperoxyl radical, eq 18 ($k_{18} = 1.2 \times 10^6$ L mol^{-1} s^{-1}).[21] Another well-characterized reaction is the

combination of two methyl radicals to form ethane, eq 19 (k_{19} = 1.6 × 10^9 L mol^{-1} s^{-1}).[22]

A mixed dialkyl peroxide formed in the oxidation of hydrocarbons by ROOH has been taken to indicate free-radical involvement.[18,23] The dialkyl peroxide arises from the reaction of alkylperoxyl radicals and carbon centered radicals. By analogy, tert-butyl methyl peroxide is suggested to form from methyl radical and tert-butyl peroxyl radical, eq 20. This should be a diffusion-controlled reaction because both species are unstable radicals.[24]

Further evidence in support of the involvement of methyl radicals comes from experiments done in the presence of O_2. Two additional products are formed, methyl hydroperoxide and formaldehyde. Methyl peroxyl radical is formed in the reaction between methyl radical with oxygen.[25] This radical could undergo a reaction analogous to eq 17 and 18 to form methyl hydroperoxide and t-BuOO$^•$: MeOO$^•$ + t-BuOOH → MeOOH + t-BuOO$^•$. Formaldehyde might then be a product of the bimolecular self-reaction of MeOO$^•$: 2 MeOO$^•$ → MeOH + CH_2O + O_2,[21] although a reviewer has noted that it might instead arise from Lewis acid (Re) catalyzed dehydration of MeOOH.

Consistent with the rate law and its [H^+]$^{-1}$ dependence, the partitioning reactions of I are, together, rate controlling. That option, which involves the breaking of covalent bonds, rather than a rate-controllling reaction between MTO and t-BuOO$^-$, is proposed for the formation of I, since precedents suggest the latter would be extremely rapid. According to that scheme, the general expression for the reaction rate is

$$\frac{d[P]}{dt} = (k_{13} + k_{14} + k_{15})\frac{K_{11}[MTO][ROOH]}{1 + k_{11}[ROOH]}\frac{k_{12}}{k_{12} + [H^+]} \tag{21}$$

Because MTO was detected throughout the reaction and $[Me(O)_3Re \cdot t-BuOOH]$ was not observed, $K_{11} < 10^2$ L mol^{-1}. Eigen and co-workers[26] report that the rate constant of proton association in an acid equilibrium reaction (k_{12}) is on the order of magnitude of 10^{10} L mol^{-1} s^{-1}. Therefore K_{12} is on the order of magnitude of 10^{-10} mol L^{-1}. With these assumptions and the experimental value for k_f of 7.4×10^{-5} s^{-1}, it follows that $k_{13} + k_{14} + k_{15} < 4 \ 10^3$ s^{-1}.

The reaction scheme consisting of eq 11-20 was further explored by simulations using the KinSim program,[27-29] a routine for generating concentration-time curves given the initial concentrations and rate constants. The mathematical algorithms are based on Gear and Runge-Kutta calculations. Certain rate constants were then optimized using the FitSim program.[30] In this manner, the agreement between the proposed reaction scheme and the experimental data could be tested. The experimental concentration-time curves for the decrease in MTO and increase in CH_3OH, $(CH_3)_2CO$, $t-BuOCH_3$, and $t-BuOOCH_3$ for three separate experiments ($[MTO]_0 = 10$mM; $[t-BuOOH]_0 = 200$ mM, 470 mM, and 600mM; $[HOTf]_0 = 100$ mM) were included as data in KinSim. Literature values for the known rate constants were used except the value of $k_{20} \sim 2 \times 10^9$ mol L^{-1} s^{-1}, a choice that is not critical to the analysis. Rough estimates for the relative ratios of rate constants for steps 13-15 were calculated from the initial rates for product buildup. The unknown rate constants were fixed and varied, accordingly, in FitSim. The actual magnitudes of k_{13}, k_{14}, and k_{15} could not be established, only the ratios could: $k_{14}/k_{13} = 1.89$, k_{15}/k_{13} = 1.61 and $k_{15}/k_{14} = 0.85$ (reliability, ± 20%). KinSim was used to simulate the total

product build up over time. The precision in measuring small concentrations of each product separately was rather low. Therefore, the buildup of the sum of product concentrations is used to represent the reaction course. Figure 3 shows that the simulated values correspond well with the experimental data, supporting the proposed mechanism.

Decomposition of MTO and t-AmOOH. To help us derive the scheme for the decomposition of methyltrioxorhenium and alkyl hydroperoxides, t-amyl hydroperoxide was employed. On the basis of the observed products, the decomposition process using t-AmOOH goes by a sequence similar to that gone by the process using t-BuOOH. There will, of course, be some minor differences in the overall scheme. The t-AmO$^\bullet$ is known to undergo β-scission at a higher rate because it forms the more stable ethyl radical.[24,31] Also, additional gaseous products (e.g. propane and ethylene) are formed in the t-AmOOH case as a result of recombination of $CH_3^\bullet$ and $CH_3CH_2^\bullet$ and the self-reaction of $CH_3CH_2^\bullet$.

The chemical products in the reactions with t-BuOOH and t-AmOOH are formed in different relative and absolute yields, as can be seen from a comparison of the data in Tables 1 and 2. A precise mass balance was not feasible since products such as methane and ethane could not be determined on a comparable basis. Not only that, but certain products (e.g., MeOH and RMe_2COMe) form directly, whereas others (e.g., Me_2CO and RMe_2COOR) result from subsequent steps.

Smurova et al. recently reported that the addition of MTO to $Ph(CH_3)_2COOH$, cumyl hydroperoxide, in chlorobenzene resulted in the heterolytic decomposition of the hydroperoxide and that <1% of the process included radical pathways.[10] The chemistry of ROOH with MTO is much different in aqueous solution than in
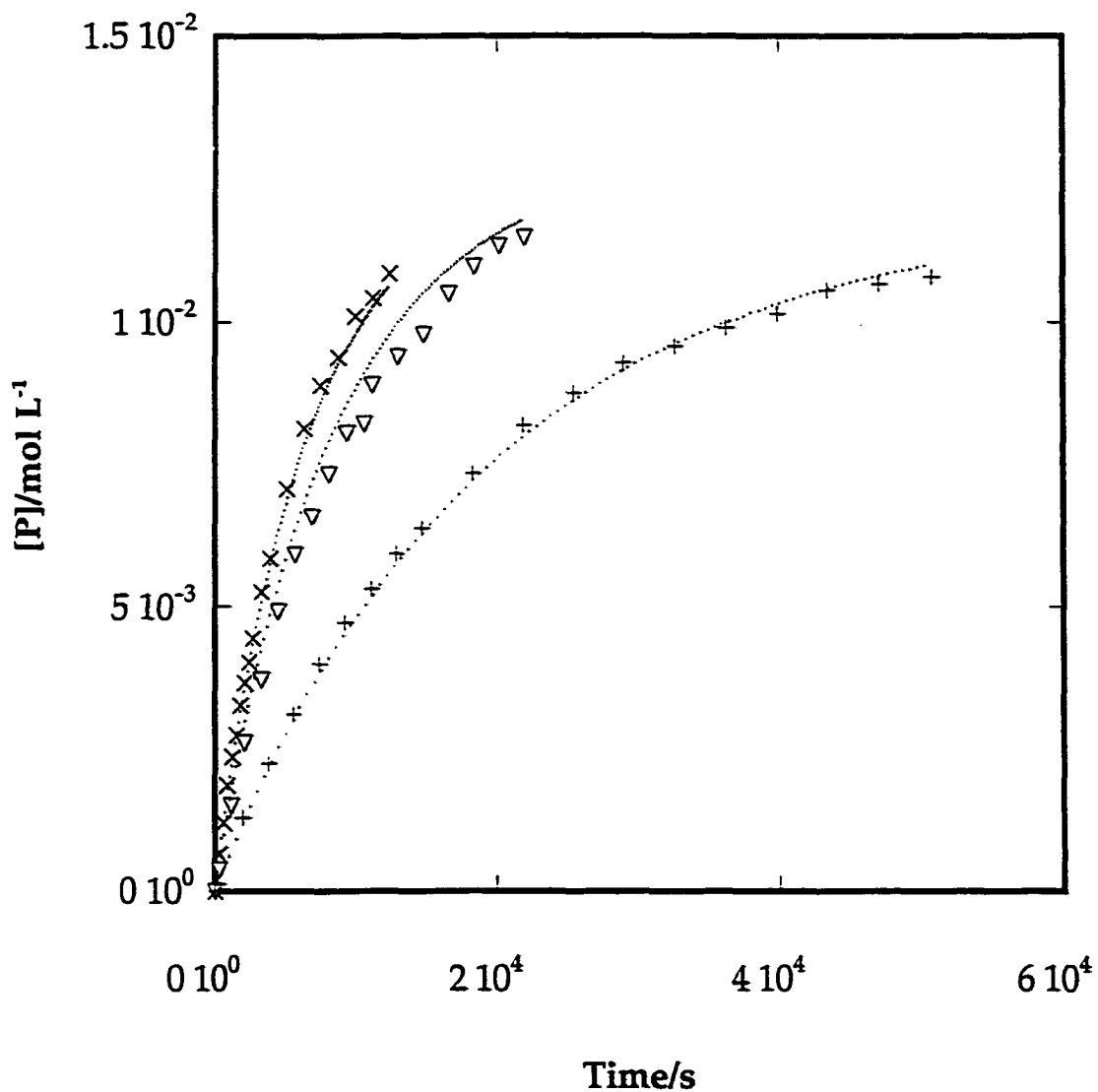
Figure 3. KinSim simulations (..........) of the buildup in total organic products for the reaction of MTO at three concentrations of t-BuOOH, 0.60 M (x); 0.47 M (∇); and 0.20 M (+). The quantity on the y axis is [P] = ([(CH$_3$)$_2$CO] + [CH$_3$OH] + [t-BuOCH$_3$] + [t-BuOOCH$_3$])/M.

chlorobenzene. In fact, the aqueous chemistry of the decomposition of CH_3ReO_3 by t-BuOOH and t-AmOOH more closely resembles the decomposition of cumyl hydroperoxide by manganese(II) and -(III) acetylacetonates in chlorobenzene.[32]

Phosphoric acid formation. This product indicates a special mechanism operates with the ternary system (MTO, t-BuOOH, and H_3PO_2). Certain radicals react with H_3PO_2 and, especially, the H_3PO_3 formed from it. This general notion finds support from the greatly enhanced rate for acetone buildup and the substantial amount of acetone formed. These findings signal the generation of additional t-BuO•, the immediate precursor of acetone in eq 16.

The methyl radical is postulated to abstract a hydrogen atom from H_3PO_3, eq 22, analogous to known reactions of H•, eq 23.[33]

$$CH_3• + H_3PO_3 \text{ (or } H_3PO_2) \rightarrow CH_4 + [P•(O)(OH)_2] \text{ or } [HP•(O)(OH)] \qquad (22)$$

$$H• + H_3PO_3 \text{ (or } H_3PO_2) \rightarrow H_2 + [P•(O)(OH)_2] \text{ or } [HP•(O)(OH)] \qquad (23)$$

The rate constants for k_{23} are 5.0×10^8 M^{-1} s^{-1} (H_3PO_3) and 4.2×10^9 (H_3PO_2).[32] Plausibly, the methyl radical abstracts H• because the bond strengths of H_2 (434.1 kJ mol^{-1})[34] and CH_4 (435 kJ mol^{-1})[35] are virtually the same. There are, of course, differences in the rates of H-atom abstraction by H• and CH_3•. For example, rate constants for a-hydrogen abstraction from alcohols are approximately 4 orders of magnitude greater with H• than with CH_3•.[36,37]

The lower limit of k_{22} can be estimated from these data to be on the order of > 10^6 mol L^{-1} s^{-1}, with an error of 1 order of magnitude, which is reasonable in that reaction 22 should be slower than reaction 23. With the long-chain approximation,[38] justified from the products formed, $k_{24} < 10^6$ mol L^{-1} s^{-1}. The phosphorus centered radicals generated in eq 22 are likely to attack the abundant hydroperoxide, eq 24, to

form additional *tert*-butoxyl radicals that lead, in turn, to acetone,[19] eq 16, and to methyl radicals, further propagating the chain.

$$H_2P^{\bullet}O_3 \text{ (or } H_2P^{\bullet}O_2) + t\text{-BuOOH} \rightarrow H_3PO_4 \text{ (or } H_3PO_3) + t\text{-BuO}^{\bullet} \qquad (24)$$

Acknowledgment.

References

1)Herrmann, W. A.; Fischer, R. W.; Scherer, W.; Rauch, M. U. *Angew. Chem. Int. Ed. Engl.* **1993**, *32*, 1157.

2)Yamazaki, S.; Espenson, J. H.; Huston, P. *Inorg. Chem.* **1993**, *32*, 4683.

3)Espenson, J. H.; Pestovsky, O.; Huston, P.; Staudt, S. *J. Am. Chem. Soc.* **1994**, *116*, 2869.

4)Hansen, P. J.; Espenson, J. H. *Inorg. Chem.* **1995**, *34*, 5839.

5)Espenson, J. H.; Abu-Omar, M. M. *Adv. Chem. Ser.* **1997**, *253*, 99.

6)Abu-Omar, M. M.; Hansen, P. J.; Espenson, J. H. *J. Am. Chem. Soc.* **1996**, *118*, 4966.

7)Zhu, Z.; Espenson, J. H. *J. Mol. Catal.* **1995**, *103*, 87.

8)Abu-Omar, M. M.; Espenson, J. H. *Inorg. Chem.* **1995**, *34*, 6239.

9)Abu-Omar, M. M.; Appleman, E. H.; Espenson, J. H. *Inorg. Chem.* **1996**, *35*, 7751.

10)Smurova, L. A.; Kholopov, A. B.; Nikitin, A. V.; Brin, E. F.; Rubailo, V. L. *Kinet. and Catal.* **1996**, *37*, 361.

11)Leslie, J. P., II; Espenson, J. H. *J. Am. Chem. Soc.* **1976**, *98*, 4839.

12)Herrmann, W. A.; Kühn, F. E.; Fischer, R. W.; Thiel, W. R.; Romão, C. C. *Inorg. Chem.* **1992**, *31*, 4431.

13)Davies, D. M.; Deary, M. E. *J. Chem. Soc. Perkin Trans.* 2 **1992**, 559.

14)Bevington, P. R.; Robinson, D. K. *Data Reduction and Error Analysis for the Physical Sciences*; 2 ed.; McGraw-Hill, Inc.: St. Louis, 1992.

15)Herrmann, W. A.; Fischem, R. W. *J. Am. Chem. Soc.* **1995**, *117*, 3223.

16)Wang, W.-D.; Espenson, J. H. *J. Am. Chem. Soc.* **1998**, *120*, 11335.

17)Suggestion made by a reviewer.

18)MacFaul, P. A.; Ingold, K. U.; Wayner, D. D. M.; Jr., L. Q. *J. Am. Chem. Soc.* **1997**, *119*, 10594.

19)Erben-Russ, M.; Michel, C.; Bors, W.; Saran, M. *J. Phys. Chem.* **1987**, *91*, 2362.

20)Bakac, A.; Wang, W.-D. *Inorg. React. Mech.* **1998**, *1*, 65.

21)Bennet, J. E. *J. Chem. Soc. Faraday Trans.* **1990**, *86*, 3247.

22)Hickel, B. *J. Phys. Chem.* **1975**, *79*, 1975.

23)Nguyen, C.; Guajardo, R. J.; Mascharak, P. K. *Inorg. Chem.* **1996**, *35*, 6273.

24)Kochi, J. K. *Free Radicals*; Ingold, K. U., Ed.; John Wiley and Sons: New York, 1973; Vol. 1, pp 1.

25)Suzuki, H.; Fukui, H.; Moro-oka, Y. *Reaction of Superoxide and t-Butylperoxide anion with Cationic Metal-Olefin Complexes*; Ando, W. and Moro-oka, Y., Ed.; Elsevier: New York, 1988, pp 269-272.

26)Eigen, M.; Kruse, W.; Maass, G.; DeMaeyer, L. *Progress in Reaction Kinetics*; Pergamon Press: Oxford, 1964; Vol. 2.

27)Barshop, B. A.; Wrenn, C. F.; Frieden, C. *Anal. Biochem.* **1983**, *130*, 134.

28)Frieden, C. *Trends Biochem Sci.* **1993**, *18*, 58.

29)Frieden, C. *Methods in Enzymology* **1994,** *240,* 311.

30)Zimmerle, C. T.; Frieden, C. *Biochem J.* **1989,** *258,* 381.

31)Walling, C. *Pure Appl. Chem.* **1967,** *15,* 69.

32)Abdalla, A. A.-S.; Ivanchenko, P. A.; Solyanikov, V. M. *Kinet. and Catal.* **1993,** *34,* 432.

33)Muratbekov, M. B.; Seriev, A. S. *High Energy Chemistry* **1983,** *17,* 432.

34)Cotton, F. A.; Wilkinson, G. *Advanced Inorganic Chemistry;* 5th ed.; John Wiley & Sons: New York, 1988.

35)Lowry, T. H.; Richardson, K. S. *Mechanism and Theory in Organic Chemistry;* 3rd ed.; Harper Collins: New York, 1987.

36)Thomas, J. K. *J. Phys. Chem.* **1967,** *71,* 1919.

37)Smaller, B.; Avery, E. C.; Remko, J. R. *J. Chem. Phys.* **1971,** *55,* 2414.

38)Espenson, J. H. *Chemical Kinetics and Reaction Mechanisms;* 2nd. ed.; McGraw-Hill, Inc.: New York, 1995.

GENERAL CONCLUSIONS

Rhenium (V) compounds have been oxidized by quinones and alkyl hydroperoxides. In Chapter 1, we have shown that quinones react with MeReO(mtp)Py and MeReO(edt)Py to form MeReO(dithiolate)Cat. This substitution reaction comes to equilibrium following a kinetic equation in which both the forward and the reverse steps are bimolecular. An octahedral intermediate, in which the pyridine and the quinone ligands are coordinated to the rhenium, has been proposed. In the case of phenanthrenequinone (PQ), the equilibrium constants have been measured and lie in the range 3.2-42.7. 3,5-di-*tert*-butyl-1,2-benzoquinone (DBQ), which has more electron density on the carbonyl oxygens, reacts with these rhenium(V) complexes much faster than PQ. The reaction with DBQ goes to completion, and therefore we could determine k_f, but not k_r. For these reactions, the forward rate constant is very dependent on the identity of the incoming quinone and only mildly dependent on the pyridine leaving group. The reverse reaction is dependent on the concentration of the incoming pyridine, but only slightly dependent on its identity. The nature of the ancillary ligand does not affect the forward rate constant, but does affect the reverse. Based on the interpretation of the kinetic data, we have proposed a mechanism, Scheme 1 of Chapter 1.

The equilibrium constants for quinone substitution, K_Q, and monomerization of dimer, K_1, correlate as thermodynamics predict. The two equilibrium reactions and constants can be combined to form a new reaction with a new equilibrium constant, K_C. K_C is independent of the identity of the pyridine ligand, and thus can be used to predict K_Q with MeReO(dithiolate)L, where L = any ligand capable of

monomerizing dimer within a specific dithiolate series. The smaller the value of K_1, the larger the value of K_Q.

In Chapter 2, we determined the rate constants for oxidation of methyldioxorhenium by *tert*-butyl and *tert*-amyl hydroperoxides. The products of these reactions are methyltrioxorhenium and the corresponding tertiary alcohol. These reactions proceed to completion with the second-order rate constants 3.71×10^4 L mol^{-1} s^{-1} (*t*-BuOOH) and 3.47×10^4 L mol^{-1} s^{-1} (*t*-AmOOH) at 25.0 °C in aqueous 1.0 M HOTf.

We also found that Re(VII) and alkyl hydroperoxides decompose each other. We have proposed a mechanism for this concurrent decomposition, Scheme 1 of Chapter 2. The alkylperoxo anion attacks the metal center to form an intermediate. This intermediate then partitions into three decomposition reactions, one of which is characterized by the homolytic cleavage of the peroxo-oxygen bonds. This leads to chemistry involving organic free radicals. The rate constants and product ratios were used to simulate this scheme. The simulations agreed well with experimental data, especially considering that radicals were involved.

ACKNOWLEDGMENTS

First I would like to extend thanks to Dr. Jim Espenson, my research advisor, for his guidance, support and patience over the years. I would also like to thank Dr. Andreja Bakac and Dr. Weidong Wang for enlightening me with their insights into chemistry. I appreciate all the assistance that the past and present Espenson group members have provided me on a daily basis. Some that deserve special mention are: Dr. Peter Metelski, Dr. Josemon Jacob, Dr. Matthew Eager, Gabor Lente, Dr. Ruili Wang, David Lahti, Ying Wang, Xiaopeng Shan, Dr. Mahdi Abu-Omar, Dr. Attila Nemes, and Dr. Timothy Zauche. I am very grateful to Brenda Smith for her endless help and friendship. My committee members also warrant mentioning for taking time out of their busy schedules to read my thesis, listen to my presentations and offer their suggestions.

My family and friends have been a constant source of encouragement. Thanks so much to Mom and Dad for letting me make my own decisions, and leading me toward the woman that I am today. My close friends deserve some super big hugs; Adie, Molly, Danielle, Maccy, Allyson and Heather; thank you for being my sounding boards on so many issues. The Special K's (Kerri and Kris) have helped keep me sane for the past few months. Jan Mitchell and my fellow yoga students have encouraged me through my journey. Thanks also to the myriad of friends that I haven't mentioned here because I don't particularly want to write a book. And last, but certainly not least, I will be eternally grateful to Dr. Derek Lane because he has helped me with calculus, computers, scientific ideas and terminology, job-hunting, writing, and personal development over the past two years.

88